DANMARKS OG GRØNLANDS GEOLOGISKE UNDERSØGELSE **RAPPORT 2021/32**

Results of CO2-flooding experiments Exp-1, Exp-2, Exp-3, and Exp-4 Greensand Project Phase 1 WP2

Dan Olsen & Samira Mohammadkhani

GEOLOGICAL SURVEY OF DENMARK AND GREENLAND
DANISH MINISTRY OF CLIMATE, ENERGY AND UTILITIES

G E U S

DANMARKS OG GRØNLANDS GEOLOGISKE UNDERSØGELSE **RAPPORT 2021/32**

Results of CO2-flooding experiments Exp-1, Exp-2, Exp-3, and Exp-4 Greensand Project Phase 1 WP2

Dan Olsen & Samira Mohammadkhani

Released 01.10.2022

GEOLOGICAL SURVEY OF DENMARK AND GREENLAND
DANISH MINISTRY OF CLIMATE, ENERGY AND UTILITIES

G E U S

Table of Contents

Summary and main conclusions

In Greensand Project Phase 1 WP2 four CO_2-flooding experiments, Exp-1, Exp-2, Exp-3 and Exp-4 were conducted on core samples from the Nini-4 well at reservoir conditions (60 ^oC, 200 bara). The experiments consisted of a complex sequence of CO_2 and formation brine injection operations aimed at evaluating the injectivity and investigating the possible reactions between supercritical CO_2, formation brine, and the greensand reservoir rock. Each experiment was conducted on a composite core sample with length approximately 15 cm, consisting of three 1.5" standard core samples.

The brine permeability measurements agree with the gas permeability determinations of the core samples from the conventional core analysis programme of Robertson Research International Ltd. (RRI). Brine permeability measurements made after CO_2-flooding operations yield the same permeability as before the CO_2-flooding operations, indicating that no significant damage is caused by the CO_2-flooding. This agrees with macroscopic visual investigations of the core samples after the experiments that do not reveal significant changes to the greensand rock.

A total of 14 CO_2 injection operations with permeability logging were conducted in the 4 flooding experiments. 11 operations used a rate of 800 ml/h, and 3 operations used a rate of 1740 ml/h. The CO_2 injection operations make a strong contrast with the brine injection operations by showing a complex permeability behaviour. The 10 injection operations that started with a fully brine-saturated state (Sw=100%) shows an initial steep rise in permeability to CO_2 from a low permeability level, which is as expected from relative permeability conditions. The permeability relationships to CO_2 deviates in two ways from the permeability relationships to brine. First, the permeability to CO_2 in the four experiments never recovers to more than between 22% and 38% of the permeability to brine. Second, in five of the 14 CO_2 injection operations a total of seven instances of abrupt, spontaneous drops in permeability were recorded, with the drops in permeability ranging from 7% to 75%. The drops in permeability were not correlated with any rig operations.

After Exp-4 the three core samples of this experiment were analysed for water saturation by Dean Stark extraction. From core holder inlet towards core holder outlet, the three samples showed water saturation results of 28%, 40%, and 65%. This shows the presence of a strong water saturation gradient within the core sample from inlet towards the outlet.

The results of the CO_2 injection operations are interpreted as being caused by channelling of CO_2 in a core sample with high water saturation. The viscosity ratio $\mu_{CO2}/\mu_w = 0.1$ caused the CO_2 to concentrate in channels, possibly more pronounced towards the outlet end of the core sample. At irregular time intervals the CO_2 flow within the core spontaneously changed to another position. The fluid density log shows production of water from the core sample through most of the CO_2 injection periods. Probably the shift in channel position was caused by changes in water distribution within the sample. Six of the seven instances of spontaneous permeability drop occurred before injecting more than 6 PV's of CO_2. Therefore, the probability of spontaneous drop in permeability is clearly greatest at the start of an injection operation when the water saturation is high.

1. Introduction

This report presents the results from four CO_2 injection experiments of EUDP Greensand Project Phase 1 WP2. The experimental work started on June 1st, 2020 and ended May 31th, 2021. The experiments are identified as Exp-1, Exp-2, Exp-3, and Exp-4 and involved injection of formation water as well as supercritical CO_2. They were optimized for evaluating the injectivity of CO_2 into the greensand lithology of the Nini West oil field of Danish North Sea.

This report is structured with an initial section that describes conditions that are common to all 4 experiments. Then follows separate descriptions of each of the 4 experiments. At the end, there are sections for discussion and conclusions.

A preliminary description of the first experiment, Exp-1, was reported in GEUS Rapport 2020/54 (Olsen et al. 2020), but the present report also includes Exp-1 because the interpretation of the experiment has changed. It is noteworthy to mention, this report is prepared under influence of significant time pressure to meet the project deadline of June 1st, 2021. Therefore, minor inaccuracies are present. However, the main conclusions are considered valid, and are not expected to change.

2. Experimental conditions and procedures

The same general experimental procedure was applied for Exp-1, Exp-2, Exp-3, and Exp-4. The description in this chapter applies to all 4 experiments. Additional information that are specific to individual experiments are given in the chapters related to each experiment.

GEUS FC Rig was used for all 4 experiments of Greensand Project Phase 1 WP2, Fig. 1. Although the rig was originally constructed for experiments with full core samples, it proved useful for the Greensand Project because of the capability to accommodate 5-liter pressure vessels for CO_2. The rig was modified during the project to provide additional volume for CO_2 by adding an extra 5-liter cylinder. The rig was also modified by adding particle traps to catch particles that moved with the fluid flow. During the first experiment, Exp-1, such particles caused experimental problems by blocking flow lines and obstructing valve operation.

Fig. 1. GEUS FC Rig used for Exp-1, Exp-2, Exp-3, and Exp-4. The horizontal core holder is seen at the upper right. In Exp-1 a vertical orientation was used for the core holder.

Determination of differential pressure is a crucial measurement in reservoir condition experiments with determination of permeability for fluids with low viscosity. The low viscosity of supercritical CO_2 necessitates the use of pressure transducers with high precision coupled with high flow rate through the core sample. The pressure transducers used have a nominal accuracy of 0.10 bar at the conditions of the experiments. However, the precision (reproducibility) is significantly better, and because the experimental procedure allowed frequent zeroing of the transducers, the differential pressure was determined with a mean error of 0.01 bar.

Table 1 gives the general conditions of all 4 experiments of Greensand Phase 1 WP2. The four experiments were conducted with the same conditions, as similar as possible, to allow direct comparison. However, to improve the informative value of the experiments, some parameters were modified in the course of the project. These modifications are mentioned under the individual experiments.

Table 1. General conditions for Exp-1, Exp-2, Exp-3, and Exp-4.

Parameter	**condition**
Formation	Frigg Member of Horda Formation
Sample material	Fine-grained glauconitic sand
Sample type	Composite 1.5" plug
Temperature at reservoir conditions	60 °C
Fluid pressure at reservoir condition	200 bara
Hydrostatic confining pressure at reservoir cond.	220 bara
Net overburden pressure (NOB) at reservoir cond.	20 to 25 bar
Flow direction	Exp-1: Vertical; Exp-2, Exp-3, and Exp-4: horizontal
Formation water	Synthetic Nini Formation brine
Injection water	Synthetic Nini Formation brine
Injection CO_2	KVGasteknik purity 4.0

Core samples

Sample material for all 4 experiments of Greensand Phase 1 WP2 was selected from a collection of 1.5” plug samples available from GEUS Core Storage Facility. The samples were originally cut and cleaned by Robertson Research International Ltd. (RRI) as part of a conventional core analysis program reported in MacDonald & Mair (2003). Conventional porosity and permeability analyses are given in MacDonald & Mair (2003). As part of the RRI analytical program the core samples were first Soxhlet cleaned with an azeotropic mixture of chloroform, methanol, and methylamine, then Soxhlet cleaned with toluene, and finally Soxhlet cleaned with methanol.

The cleaning state of the samples for Exp-1 was checked by a short Soxhlet cleaning with methanol, where no chloride ions were found. After that, no further cleaning of the samples for any of the experiments was conducted. The RRI cleaning of the samples is considered thorough and qualified.

Since the RRI samples were in a loosely consolidated state, with sand grains being lost from the samples every time they were handled, conventional porosity and permeability analyses were not conducted at GEUS. Instead, the data from the RRI report was used. It was generally considered that the samples should be used with a minimum of handling.

Nini Formation brine

The formation brine used in all 4 Greensand Project Phase 1 WP2 experiments was synthetic brine, prepared from the average composition of several water analyses from the greensand reservoirs of the Siri canyon. The average composition was compiled by Niels Schovsbo, GEUS (Olsen et al., 2020). To avoid precipitation of insoluble minerals, the contents of Ba^{2+}, HCO_3^-, and Fe_{tot} were reduced in the recipe used for brine preparation. The contents of Cl^- was adjusted to stoichiometry as well. The average composition of Nini brine and the brine used in the experiments of the present report are shown in Table 2. The latter analysis is referred as Nini Formation brine. Formation brine was always degassed before being used in the experiments to avoid unwanted oxidation during the experiments.

The viscosity of Nini Formation brine was calculated to be 0.565 cP at 200 bara and 60 °C by the equations of Kestin et al (1978). This viscosity value is used throughout the present report.

Table 2. Nini Formation brine used in Project Greensand Exp-1. See Olsen et al. (2020).

Component or Parameter	Mean composition of produced water from Nini (Schovsbo)	Synthetic formation water used in WP2 experiments: Nini Formation brine
Na^+ (mg/l)	29300	29300
Ca^{2+} (mg/l)	4800	4800
Mg^{2+} (mg/l)	1027	1027
K^+ (mg/l)	211	211
Ba^{2+}(mg/l)	123	20
Fe_{tot} (mg/l)	0.9	0.0
Sr^{2+} (mg/l)	602	602
Cl^- (mg/l)	57900	57351
SO_4^{2-} (mg/l)	6.3	6.3
HCO_3^- (mg/l)	100	10
Salinity (wgt%)	n.a.	8.79
Density (g/ml) @ 1 atm, 23 °C (1)	n.a.	1.063
Density (g/ml) @ 200.0 bara, 60 °C (2)	n.a.	1.053
Viscosity (cP) @ 200.0 bara, 60 °C (3)	n.a.	0.565

(1) Fluid density measured at GEUS with Paar DMA 35.
(2) Fluid density measured at GEUS with Paar DMA HPM.
(3) Brine viscosity at reservoir conditions calculated from Kestin et al. (1978)

Determination of differential pressure in rig tubing

The FC Rig of GEUS was originally constructed for flooding experiments on samples with low permeability. In such experiments, the differential pressure in the rig tubing is of minor concern. This is not the case for experiments with high permeability samples. In the FC Rig, the two points where the differential pressure transducer connects to the flow lines are situated relatively far from the ends of the core sample. In Exp-3 and Exp-4, the distance from the upstream connection point to the inlet end of the core sample was 150 cm, while the distance from the downstream connection point to the outlet end of the core sample was 91 cm. The tubing involved is mainly 1/8" tubing with inner diameter of 1.4 mm. These conditions cause a significant differential pressure to be present in the tubing at the flow conditions of the experiments of the present report. To correct for this, the differential pressure in the tube connections was determined in two flow experiments where the conditions were exactly as in Exp-3 and Exp-4, i.e. 200 bara fluid pressure and 60 °C. The flow rates were 100 ml/h for brine and 800 and 1740 ml/h for CO_2, which are the rates used in Exp-3 and Exp-4. Furthermore, the two experiments used the same core holder as Exp-3 and Exp-4, but only without any core sample. Table 3 gives the measured differential pressure of the tube connections.

The differential pressure readings of Exp-3 and Exp-4 are corrected with the values given in column "Average differential pressure" of Table 3.

Table 3. Differential pressure of rig tubing between connections to differential pressure transducer.

Flow conditions	Exp-A differential pressure with empty core holder (bar)	Exp-B differential pressure with empty core holder (bar)	Average differential pressure (bar)
Brine flow 100 ml/h	0.0027	0.0019	0.0023
CO_2 flow 800 ml/h	0.0037	0.0052	0.0045
CO_2 flow 1740 ml/h	0.0165	0.0194	0.0180

Samples from particle traps of produced fines

After all four experiments, the contents of the particle traps of the rig were extracted. In Exp-1, only the two external particle traps were existed, as the internal particle traps had not yet been installed. In Exp-2, Exp-3, and Exp-4, the fines from both the two external traps and the two internal traps were extracted.

The contents of traps in Exp-1 were filtered through 8 micron filters and washed with de-ionized water to remove any possible salt. The contents of traps in Exp-2, Exp-3, and Exp-4 were treated the same as Exp-1 with the difference that filters with 0.45 micron size were used.

Fig. 2 shows the contents of the traps of Exp-4. Trap-1 did not contain any fines. Trap-2 and Trap-3 each contained approximately 0.2 g of particles, which clearly was material that was detached from the adjacent core sample. Trap-4 contained 0.008 g of particles, that had travelled 42 cm downstream from the core sample through the rig tubing carried by the fluid flow.

The contents of the traps in Exp-2 and Exp-3 were similar to Exp-4. The contents of the traps are currently considered for mineralogical characterization, in particular the contents of the Trap-4 situated 42 cm downstream to the core sample, as the particles of this trap clearly were able to travel a significant distance during the flooding experiments.

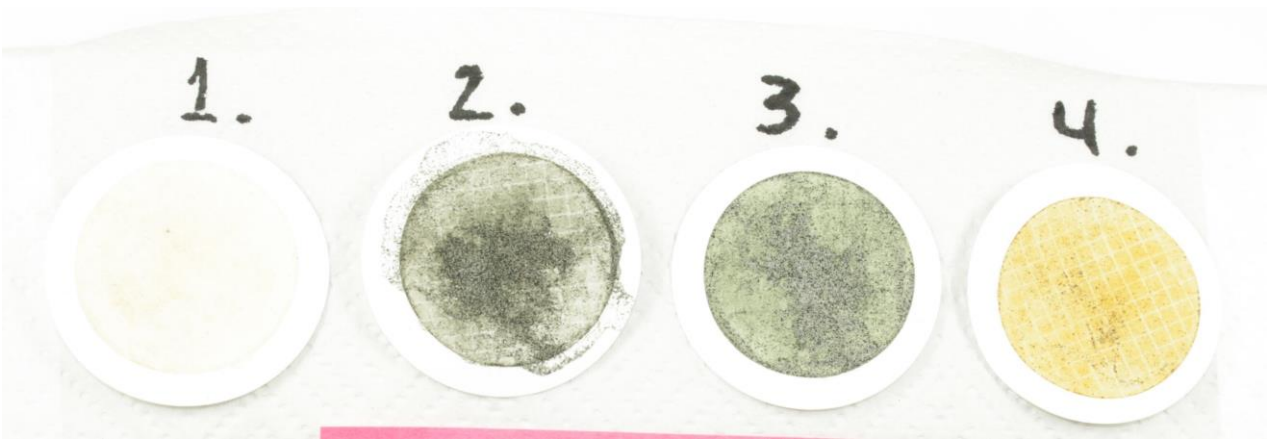

Fig. 2. Contents of particle traps for Exp-4. Sample-1, 18 cm upstream from core inlet, 0.000 g. Sample-2 adjacent to inlet end of core sample, 0.101 g. Sample-3 adjacent to outlet end of core sample, 0.125 g. Sample-4, 42 cm downstream from core sample, 0.008 g.

2.1 Experiment Exp-1

Core samples

Three 1.5” plug samples with RRI identification numbers #90, #91, and #94 were selected for experiment Exp-1. Fig. 3 shows the dry state of the three samples before starting Exp-1. Table 4 gives the core samples characteristics. The average gas permeability for the samples is 1177 mD, the total length is 15.04 cm and the pore volume is 56.3 ml.

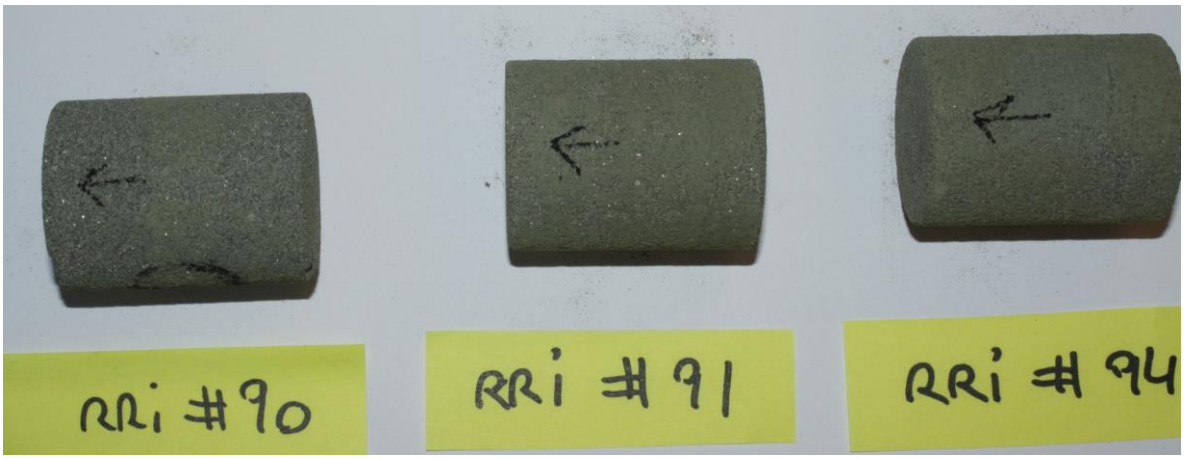

Fig. 3. Plug samples used in experiment Exp-1

Table 4. Exp-1 samples characterizations.

Sample Id.			RRI						
	Depth	Orient	Por	Gas perm	Gr. dens.	Diam.	Length	GeomBV	PV
	(MD, m)		(%)	(mD)	(g/ml)	(cm)	(cm)	(ml)	(ml)
90	1774.66	Horiz.	34.0	1160	2.69	3.70	5.01	53.87	18.315
91	1775.04	Horiz.	35.0	1180	2.69	3.70	5.00	53.76	18.816
94	1776.04	Horiz.	35.4	1190	2.70	3.70	5.03	54.08	19.145
Average or cumulative value			34.8	1177	2.69	3.70	15.04	161.71	56.277
Std. dev			0.72	15	0.006	0.00			

Experimental set-up

The three plugs (#90, #91, and #94) were saturated with Nini Formation brine, and were mounted as a composite core sample in a hydrostatic core holder. A steel filter with 1 mm mesh size was placed at each end of the composite core sample before mounting the core holder in GEUS FC Rig. A particle trap was installed downstream to the vertical core holder, and another particle trap was installed upstream to the core holder. Fig. 1 shows GEUS FC Rig that was used for Exp-1. Please note that in Exp-1 the core holder was in a vertical position, while in Fig. 1 a horizontal core holder is shown.

Reservoir condition experiments

Summary of operations during core flooding Exp-1:

1. Mounting core holder with 3 greensand samples in GEUS FC Rig
2. Establishing reservoir conditions
3. Measurement of initial permeability to brine @ 800 ml/h
4. 1st CO_2 flooding in upwards direction @ 800 ml/h, 33.5 PV's injected in 2.4 hours
5. 1st Brine flooding in upwards direction @ 100 ml/h, 2.6 PV's injected in 1.5 hours
6. 2nd CO_2 flooding in upwards direction @ 800 ml/h, 21 PV's injected in 1.5 hours
7. 2nd Brine flooding in upward direction @ 100 ml/h, 0.5 PV's injected in 0.25 hour
8. No-flow condition for 17 hours
9. Continue 2nd Brine-flooding in upwards direction @ 100 ml/h, 3.0 PV's injected in 1.6 hour
10. 3rd CO_2 flooding in upwards direction @ 800 ml/h, 17.4 PV's injected in 1.2 hours
11. Work to change flow direction
12. 3rd CO_2 flooding in downwards direction @ 800 ml/h, 6.0 PV's injected in 0.4 hours
13. Flooding stopped when CO_2 supply ran empty
14. Depressurization and cooling of reservoir rig
15. Dismounting core holder from rig, dismount plug samples from core holder.

Measurement of initial permeability to brine

Permeability to brine was measured by flooding the core samples with Nini Formation brine at 800 ml/h, cf. Fig. 4. A brine permeability of 978 mD was measured. The mean value of the 3 gas permeability determinations of RRI is 1177 mD (Table 4). Because brine permeability determinations are usually lower than gas permeability determinations on the same sample (Bloomfield & Williams, 1995), the permeability determinations are considered to agree.

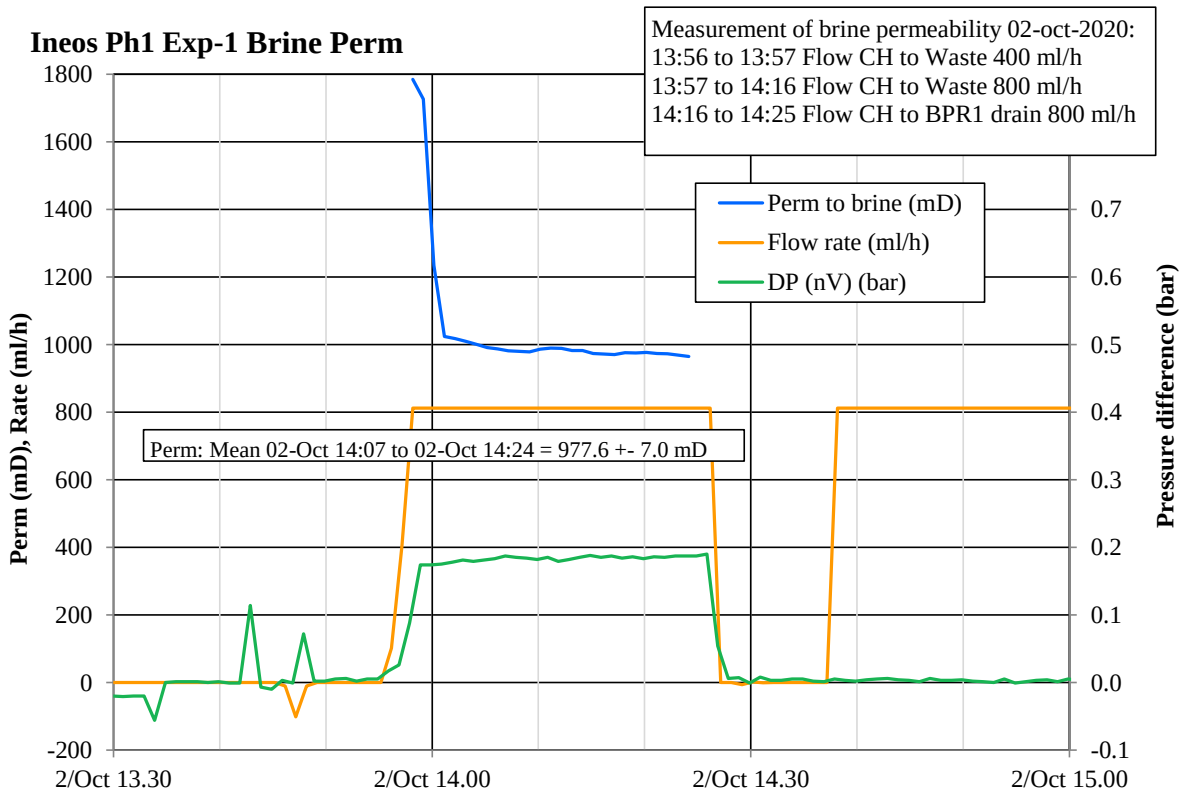

Fig. 4. Experiment Exp-1. Initial permeability to brine.

Flooding with CO_2 and brine

Fig. 5 gives an overview of the injection periods of Exp-1. A total of 85.4 pore volumes of fluid (PV's) were injected with alternating injection of CO_2 and Nini Formation brine. The flooding operations covered two days, with a 17 hour period without flow during the night between the two days. The period without flow took place at the end of a short formation water flooding, to allow the core sample to react with formation water saturated with residual CO_2 in the period without flow. During the flooding operations the maximum fluid pressure variation was ± 1.2 bar, and the maximum temperature variation was ± 0.09 °C. Therefore, pressure and temperature are considered constant at 200 bara and 60 °C.

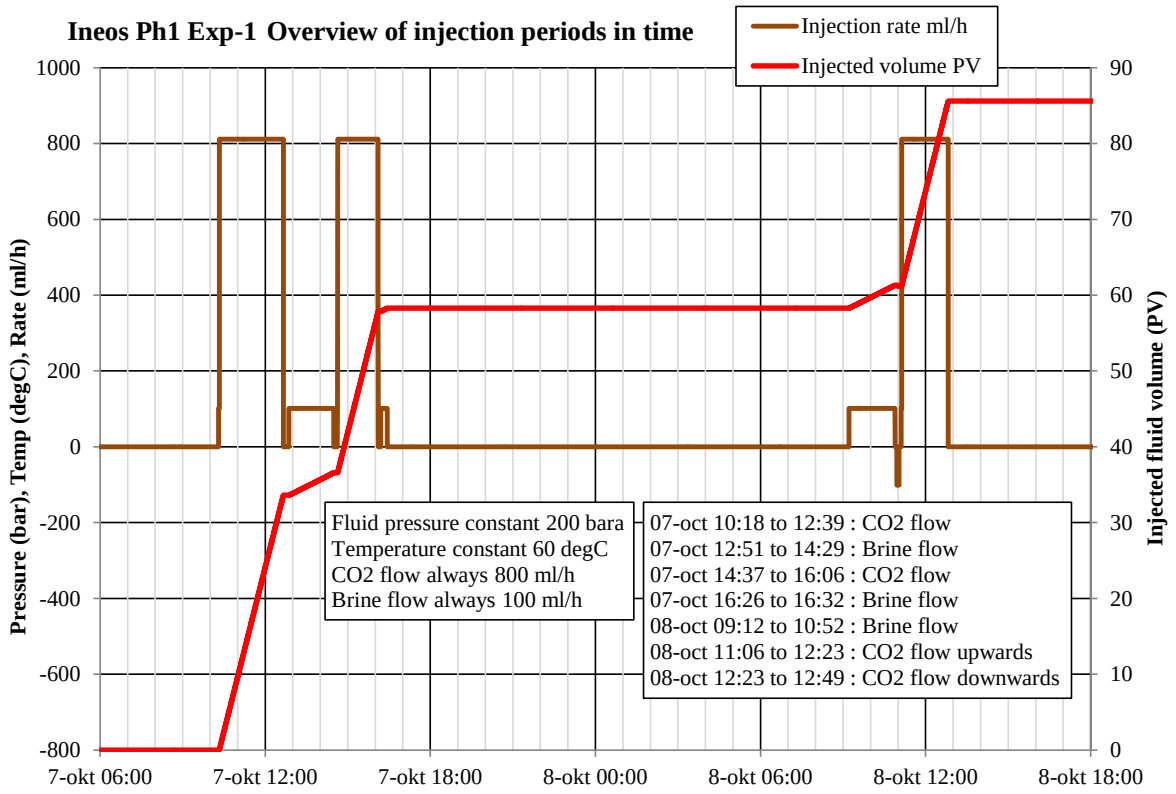

Fig. 5. Experiment Exp-1. Overview of injection periods.

Fig. 6 shows the flooding operations plotted against injected pore volumes. The plot shows three periods with CO_2 injection separated by two periods with brine injection. The first period with brine injection contains a short period from PV 36.1 to PV 36.4 without ΔP data. The missing data occurs towards the end of the brine injection period, but the ΔP data acquisition was restored shortly before the end of injection period, and valid permeability data are seen as a short blue line at PV 36.4 as 450 mD.

The second brine injection period contains the 17 hours break without flow at PV 58.1. When flow was restarted, it took some time before ΔP come to equilibrium. In the disequilibrium period the calculated permeability is erroneous and therefore the permeability spike at PV 58.1 should be disregarded. The same should apply to all other permeability anomalies associated with flow rate changes.

The two first periods with CO_2 flooding show some similarity. At the beginning of each CO_2 flooding period the permeability increases steeply, followed by a slower and slower rise in permeability. The first CO_2 flooding period ends at a stable permeability of 180 mD, while the second permeability period ends at a stable permeability of 200 mD. Both permeability values are much lower than the pure brine permeability of 978 mD shown in Fig. 4.

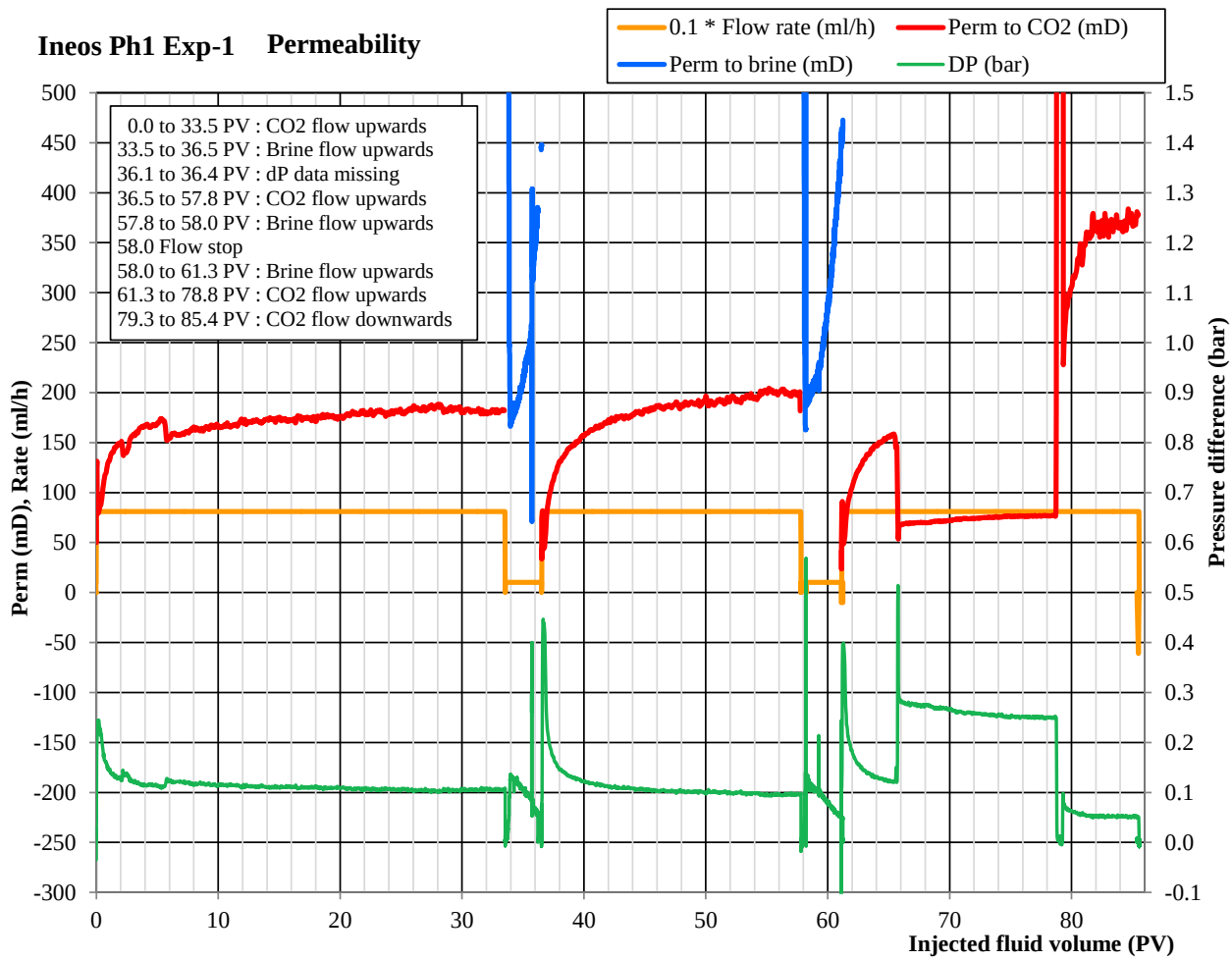

Fig. 6. Experiment Exp-1. Flooding operations overview.

A distinction of the first CO_2 flooding period is two events at PV=2.2 and PV=5.8, where the permeability shows spontaneous, abrupt drops. These drops are addressed in the section with discussion.

The two brine injection operations are very similar, showing steep increases in permeability, however the permeability curves do not reach stability. For both periods, the brine injection reaches a brine permeability of approximately 450 mD, but the brine permeability would undoubtedly have increased, if brine injection had been continued. The brine injection periods were limited by the volume of brine in the brine supply cylinder.

The third period with CO_2 injection behaved different from the first two CO_2 injection periods. Initially, the CO_2 permeability increased like the second CO_2 injection period. However, at PV 65.7 a sharp drop in permeability occurred with permeability changing abruptly from approximately 160 mD to 50 mD. The drop in injectivity cannot be related to any external cause. After the drop in permeability, the permeability quickly recovered to 68 mD, and then at a slow rate to 72 mD. The experiment operator observed the development and decided to reverse the flow direction in the core sample. The flow reversal operation took place from PV 78.8 to PV 79.3 (Fig. 6). During the flow reversal operation, the core sample had no flow. When flow was resumed in reverse direction, the permeability immediately recovered to a permeability level that was higher than in the first two CO_2 injection periods. Furthermore, the permeability continued to increase, and reached 375 mD at the end of the experiment. The CO_2 injection stopped when the CO_2 supply was empty which occurred at PV 85.4 (Fig. 6). At this time, the permeability to CO_2 was still slowly rising.

Fig. 7 shows a close-up of the permeability drop that occurred at PV 65.7.

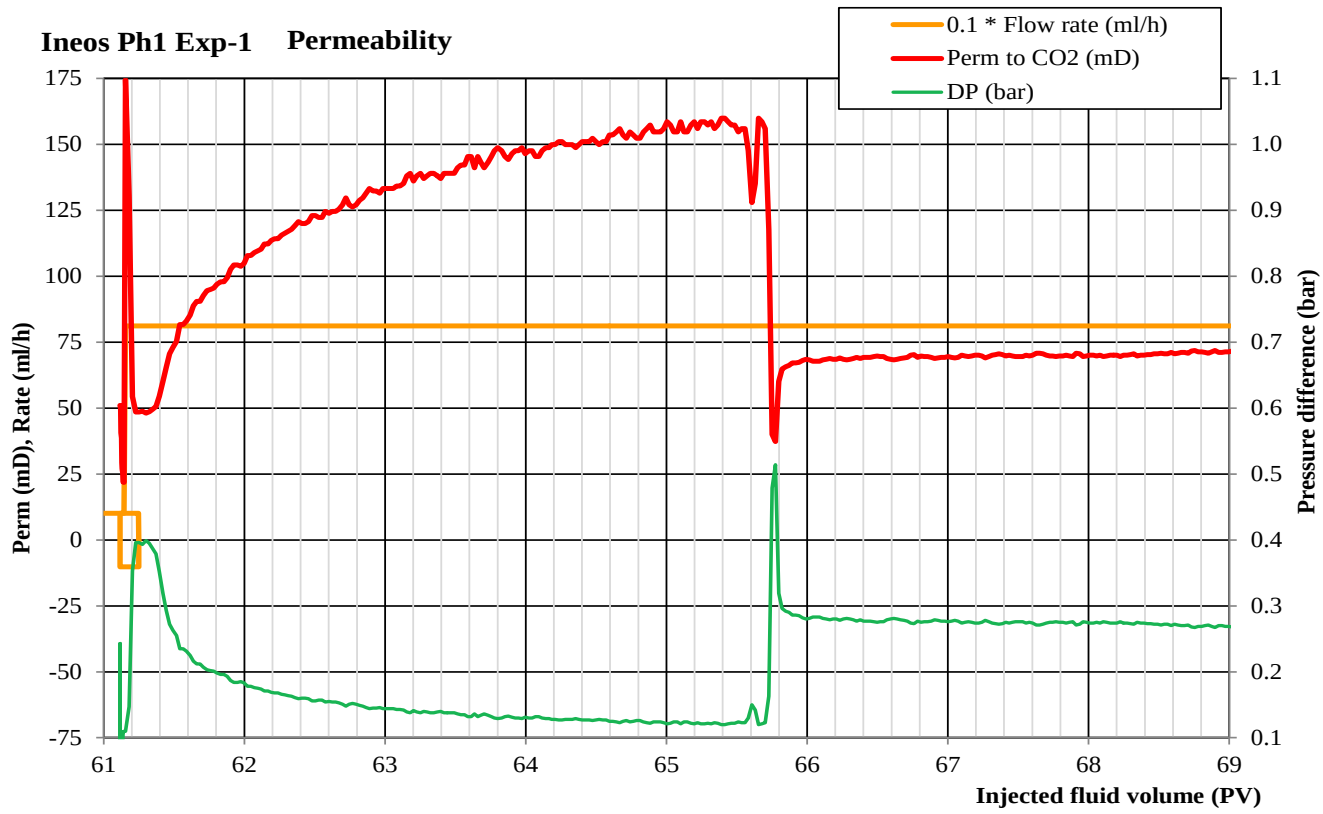

Fig. 7. Experiment Exp-1. 3rd CO_2 injection operation. Drop in injectivity at PV 65.7.

The sharp increase in ΔP takes place in only 0.048 PV, equivalent to injection of 2.8 ml of CO_2. The following quick increase in injectivity took place at the same speed, within 0.048 PV. The logging interval was 6 seconds, equivalent to 0.024 PV at rate 800 ml/h.

An incident occurred during the first brine flooding period, where NOB abruptly decreased from 20 to 5 bar, with derived fluctuations in ΔP cf. Fig. 8. The cause of the incident is not clear. The automatic NOB control program of the reservoir rig quickly restored NOB to the nominal value of 20 bar, but the incident did cause a shift in the brine permeability trend. The increasing trend in the brine permeability curve was not disturbed.

A similar drop in NOB was recorded 5 hours later at a time where no flow took place. This time NOB decreased to 6.6 bar, and again recovered by the automatic NOB control program.

The cause of the two incidents of NOB decrease is not clear. The automatic NOB control program has been used for many years and is considered reliable. Apart from the shift in brine permeability trend, the incidents did not appear to cause changes to Exp-1.

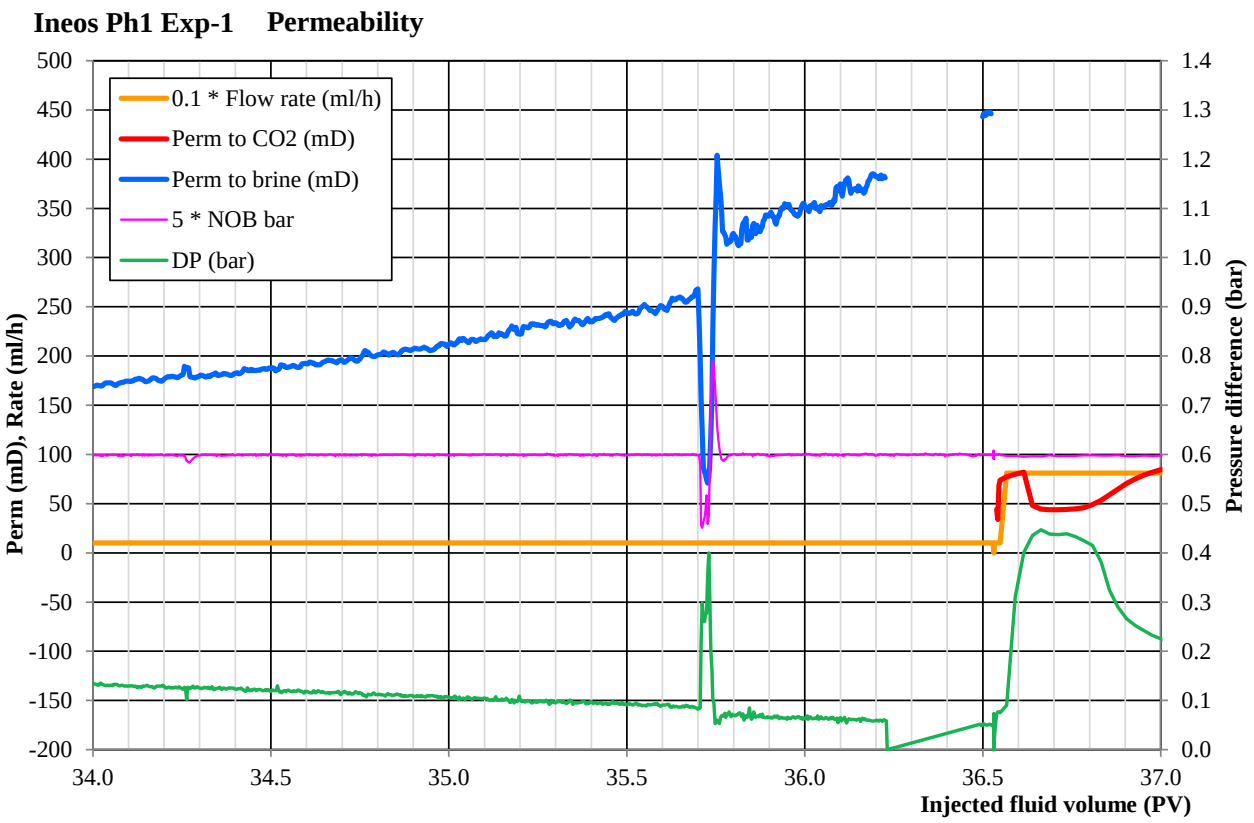

Fig. 8. Experiment Exp-1. Drop in NOB at PV 35.7.

Rock mechanical aspects of experiment

During Exp-1, the position of the core holder floating piston was measured 5 times, Fig 9. The measurements were made with a simple electronic calliper, with an estimated uncertainty of 0.04 mm. To make the measurements it was necessary to open the rig oven, and therefore the measurements were only made when the resulting temperature fluctuations did not disturb the flooding operations.

During establishment of reservoir conditions, from September 23rd to 25th, the floating piston retracted approximately 0.1 mm. This is common during establishment of reservoir conditions, and probably mainly reflects settling of the core holder end pieces. In the period at reservoir conditions before the CO_2-flooding, no significant movement of the core holder piston was seen, as the recorded positions are within measuring uncertainty.

During the CO_2-flooding period, from October 6th to 9th, the core holder piston retracted approximately 0.1 mm, which is considered above the measuring uncertainty. It thus seems that the CO_2- and brine-floodings effected a slight compaction of the core sample, with a length reduction of approximately 0.07%.

After experiment Exp-1, the core samples appeared unaffected by the flooding experiments. The samples are currently being investigated for effects of the flooding experiments on porosity, permeability, and mineralogical changes.

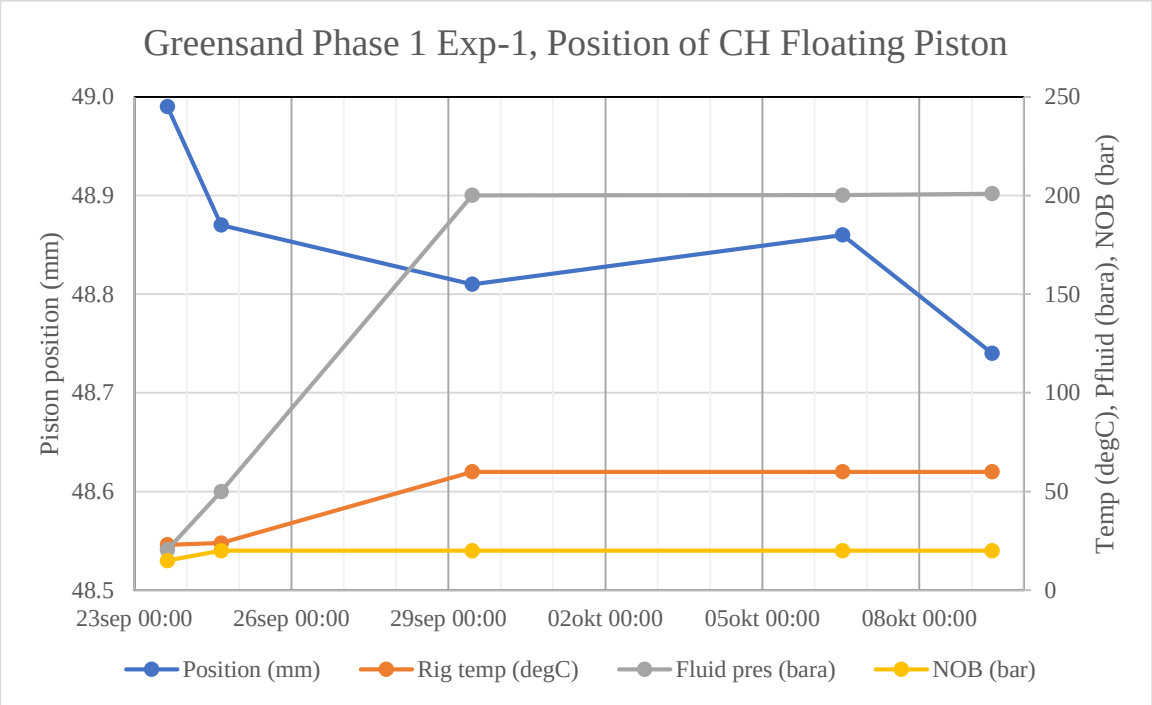

Fig. 9. Experiment Exp-1. Position of core holder floating piston. CO_2 flooding operations took place October 7th to 8th. Estimated uncertainty of measurements is 0.04 mm.

2.2 Experiment Exp-2

Core samples

RRI samples with numbers #96, #97, and #99 were selected for experiment Exp-2 (Fig. 10). As it shows in Fig. 10, sample #97 was wrapped in a heat shrinkable sleeve and contained filters as received from RRI. The sample was unwrapped before drying and using in Exp-2. Table 5 gives the properties of the samples. The average gas permeability of the samples was 1310 mD, the total length was 15.04 cm and pore volume of 56.4 ml.

Fig. 10. Plug samples used in experiment Exp-2

Table 5. Exp-2 sample characterization.

Sample Id.			RRI						
	Depth	Orient	Por	Gas perm	Gr. dens.	Diam.	Length	GeomBV	PV
	(MD, m)		(%)	(mD)	(g/ml)	(cm)	(cm)	(ml)	(ml)
96	1776.66	Horiz.	34.6	1420	2.69	3.70	5.00	53.73	18.590
97	1777.04	Horiz.	35.5	1230	2.70	3.70	5.02	54.02	19.177
99	1777.66	Horiz.	34.6	1280	2.70	3.70	5.02	53.95	18.668
Average or cumulative value			34.9	1310	2.70	3.70	15.04	161.70	56.435
Std. dev			0.52	98	0.006	0.00			

Experimental set-up

The three plugs (#96, #97, and #99) were saturated with Nini Formation brine, and were mounted as a composite core sample in a hydrostatic core holder. Two steel filters with 1 mm mesh size were placed at each end of the composite core sample. The possibility of blocking the tube lines by fines was concluded in Exp-1, despite the presence of the particle traps outside the core holder. To prevent further blockage, two particle traps with length of 8 mm were put inside the core holder in both ends of composite core, stick to the steel filters. Fig. 11 shows one of the particle traps used to prevent movement of fines in the rig tubing during the experiment.

The core holder was mounted in GEUS FC Rig., the same rig and arrangement as seen in Fig. 1. Two other particle traps were used in the upstream and downstream of the flow right before and after the core holder. The core holder in this experiment has horizontal position.

Fig. 11. Exp-2. Particle traps used in the core holder in both ends of composite core.

Reservoir condition experiments

Five injection cycles of supercritical CO_2 and Nini formation brine were conducted in Exp-2. The second CO_2 injection was conducted with lower flow rate to increase the time of injection. Summary of operations during core flooding Exp-2 are as follow:

1. Mounting core holder with 3 greensand samples in GEUS FC Rig
2. Establishing reservoir conditions
3. Measurement of initial permeability to brine @ 100 ml/h
4. 1st CO_2 injection from fixed end of core holder towards floating end @ 800 ml/h, 35.44 PV's injected in 2.5 hours
5. 1nd brine injection in the same direction @ 100 ml/h, 4.94 PV's injected in 2.8 hours
6. 2nd CO_2 injection in the same direction @ 10 ml/h, for 115.73 hours equal to 20.71 PV's
7. 2rd brine injection in the same direction @ 100 ml/h, 6.74 PV's injected in 3.8 hours
8. No-flow condition for 18.2 hours
9. 3rd CO_2 injection in the same direction @ 800 ml/h, 29.77 PV's injected in 2.1 hour
10. 3th brine injection in the same direction @ 100 ml/h, 6.74 PV's injected in 3.8 hours
11. Failed attempt to 4th CO_2 injection. The injection continued at 800 ml/h for 1 hour equal to 14.18 PV's, but the pressure drop (ΔP) had lots of fluctuations and could not be read correctly by differential pressure transducers.
12. No-flow condition for 14.44 hours. Work to solve the problem in CO_2 injection failure.
13. 4th CO_2 injection at 800 ml/h, for 1.2 hours equal to 17 PV's after solving the problem
14. 4th brine injection at 100 ml/h, 4.1 PV's injected in 2.3 hours
15. 5th CO_2 injection at 800 ml/h, 29.79 PV's injected in 2.1 hours
16. 5th brine injection at 100 ml/h, 4.6 PV's injected in 2.6 hours
17. Injection operations stopped
18. Depressurization and cooling of reservoir rig
19. Dismounting core holder from rig, dismount plug samples from core holder.

Initial measurement of brine permeability

Permeability to brine was measured by flooding the core samples with Nini Formation brine at 100 ml/h, shown at Fig. 12. Brine permeability for this operation is 1030.1 mD and slightly higher than the permeability to brine in Exp-1, 977.6 mD. The difference agrees with the higher gas permeability for the samples in Exp-2, 1310 mD in comparison with samples in Exp-1, 1177 mD.

Fig. 12. Experiment Exp-2. Initial permeability to brine.

Flooding with CO_2 and brine

After brine permeability measurement, CO_2 and formation brine were injected in five cycles in Exp-2. An overview of the flooding operations is shown in Fig. 13. CO_2 was injected first at 800 ml/h in the first cycle for 35.44 PV's followed by formation water injection. In the second cycle, CO_2 was injected at 10 ml/h for 20.71 pore volumes. Since the flow rate was low, the pressure drop across the core was subsequently low and could not be detected by available differential pressure transducer. The reason for injecting the CO_2 at low flow rate was to increase the time of CO_2 injection and subsequent contact of rock surface with CO_2. The second flooding cycle was finished following by formation brine injection.

CO_2 was flooded successfully in the third cycle as well as formation brine injection. CO_2 was injected for 29.77 PV's at the flow rate of 800 ml/hr in this cycle. Brine was injected after this CO_2 injection as well. The injection of brine in each cycle in Exp-2 was not sufficient enough to reach the constant pressure drop across the core samples.

Before starting the fourth cycle, CO_2 was injected to the core to increase the possible reactions. After 15 hours, in the fourth cycle, the attempt to inject CO_2 was failed. The failure was observed when the injection pressure was increased following by reduction in receiving pressure. In the next attempt, the injection was continued at 800 ml/h flow rate for 14.18 PV's but the fluctuations in differential pressure transducer reading did not allow proper calculation of permeability.

At this time, the experiment was stopped to be able to find the reason for the problems and consequently solve them. The problem was found by injecting brine through different tube lines, which finally located a blockage in the Paar density meter. This blockage in the density meter was caused by precipitation of solid minerals within the flow liners of the density meter, possibly enhanced by accumulation of moving fine particles. After Exp-2 the density readings of the density meter had changed significantly, resulting in too high density readings. This error state could not be corrected by flushing, but treatment with hydrochloric acid did result in more normal density readings. This is indicates that solid minerals precipitated inside the density meter in Exp-2. From this time in Exp-2, the density meter was bypassed by the fluid flow, and therefore, density measurements are not available.

After putting the density meter out of the flow line, a successful CO_2 injection was conducted at 800 ml/h for 17 PV's. Formation brine was injected afterward. The fifth cycle was started with another failure that was resolved by reversing the flow and removing the possible blockage in the valves or lines. It is not clear where the blockage happened at this time. CO_2 was injected successfully afterward for 29.79 PV's at 800 ml/h in the fifth cycle. The experiment was ended at this cycle by flooding formation brine.

Apart from the incident happened in the beginning of fourth and shortly before fifth CO_2 flooding, and low flow rate in CO_2 flooding at cycle 2, the permeability was measured successfully for the cycles 1, 3, 4 and 5. The CO_2 was not flooded enough to reach the stable pressure drop across the core in all the CO_2 flooding sequences. In the first CO_2 flooding after 35.44 PV's of injection reached the stable pressure drop and permeability was measured as 354.8 mD.

Fig. 13 shows the sequence of flooding operations in experiment Exp-2. The flow rate is divided to 10 to fit the margin of the figure. Fluid pressure, pressure difference across the core and permeability curves are shown in this figure. The density measurements stopped due to blockage of lines close or in the interior part of the density meter at around PV=125.

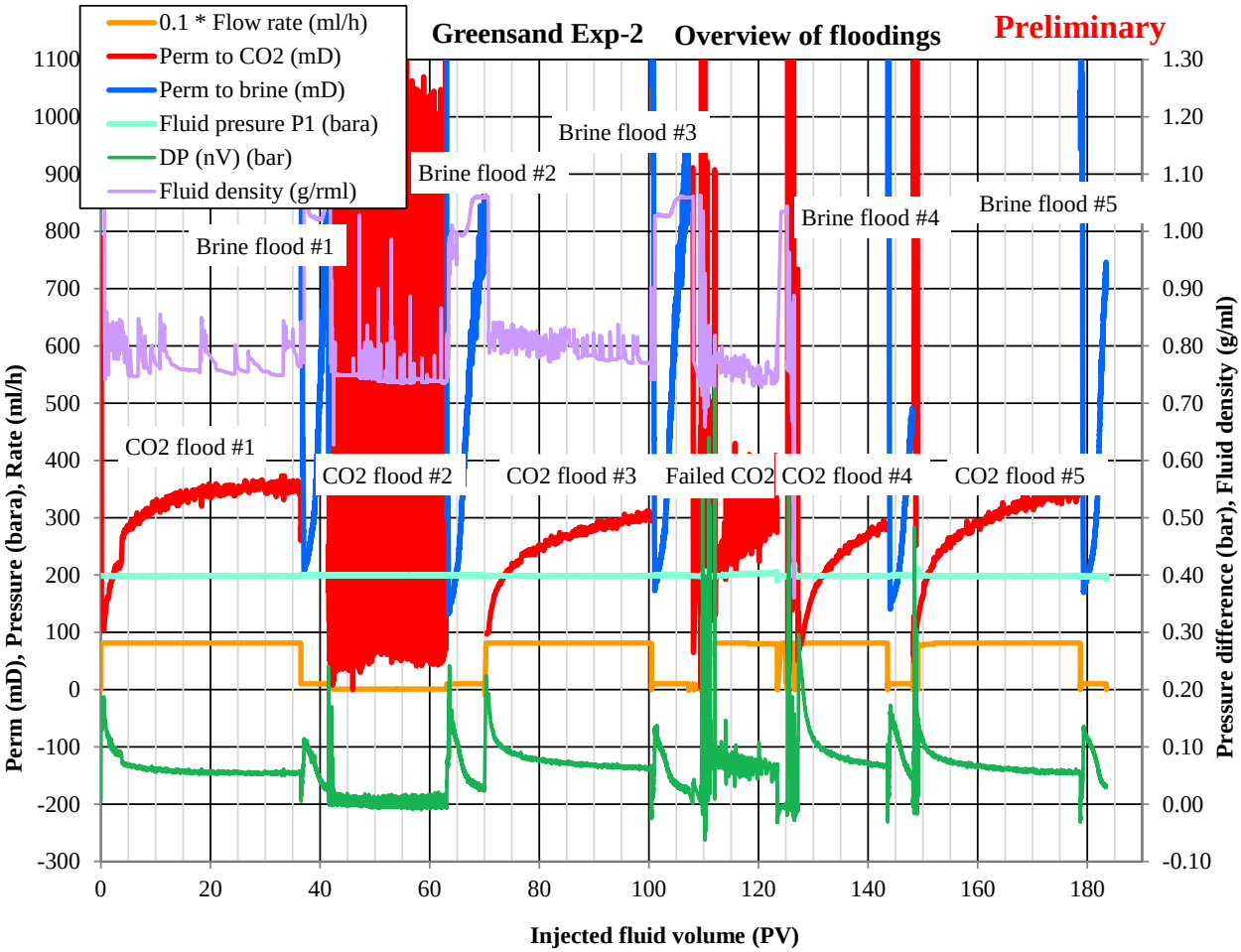

Fig. 13. Experiment Exp-2 flooding operation.

The entire cyclic flooding of CO_2 and formation brine in Exp-2 took place in 8 days. The low flow rate CO_2 flooding took the most time (around 5 days). Fig. 14 shows the period of first cycle of CO_2 injection after brine permeability measurement and the low flow rate CO_2 flooding with brine flooding in between. Since the flow rate is low in the second cycle, the pressure drop across the samples could not be measured, and it is as low as zero.

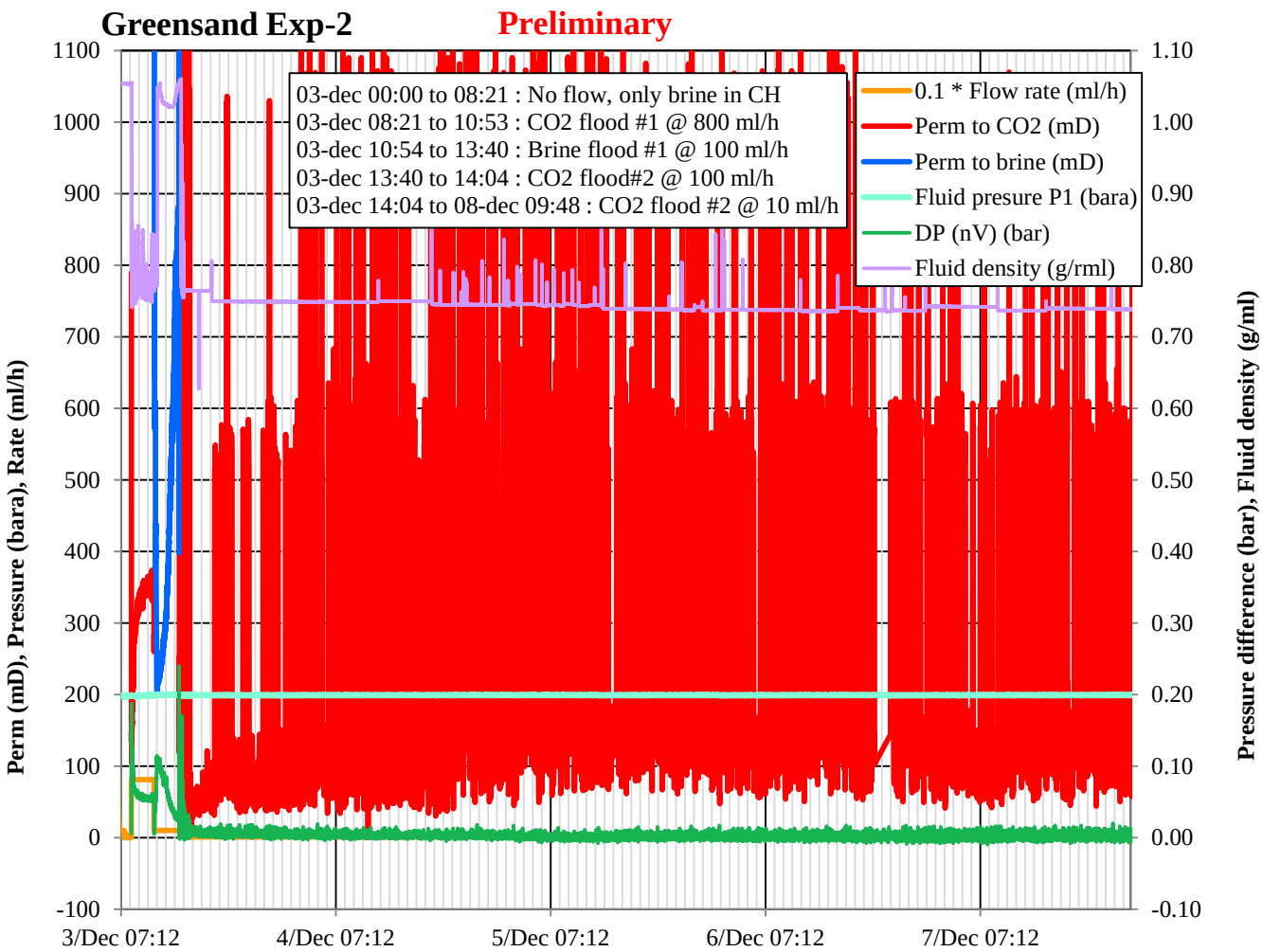

Fig. 14. Experiment Exp-2 first two CO_2 injection operations and the brine injection in between.

Failure of CO_2 injection on 10th of December is shown in Fig. 15. The fluctuations in differential pressure measurements are clearly shown in this figure.

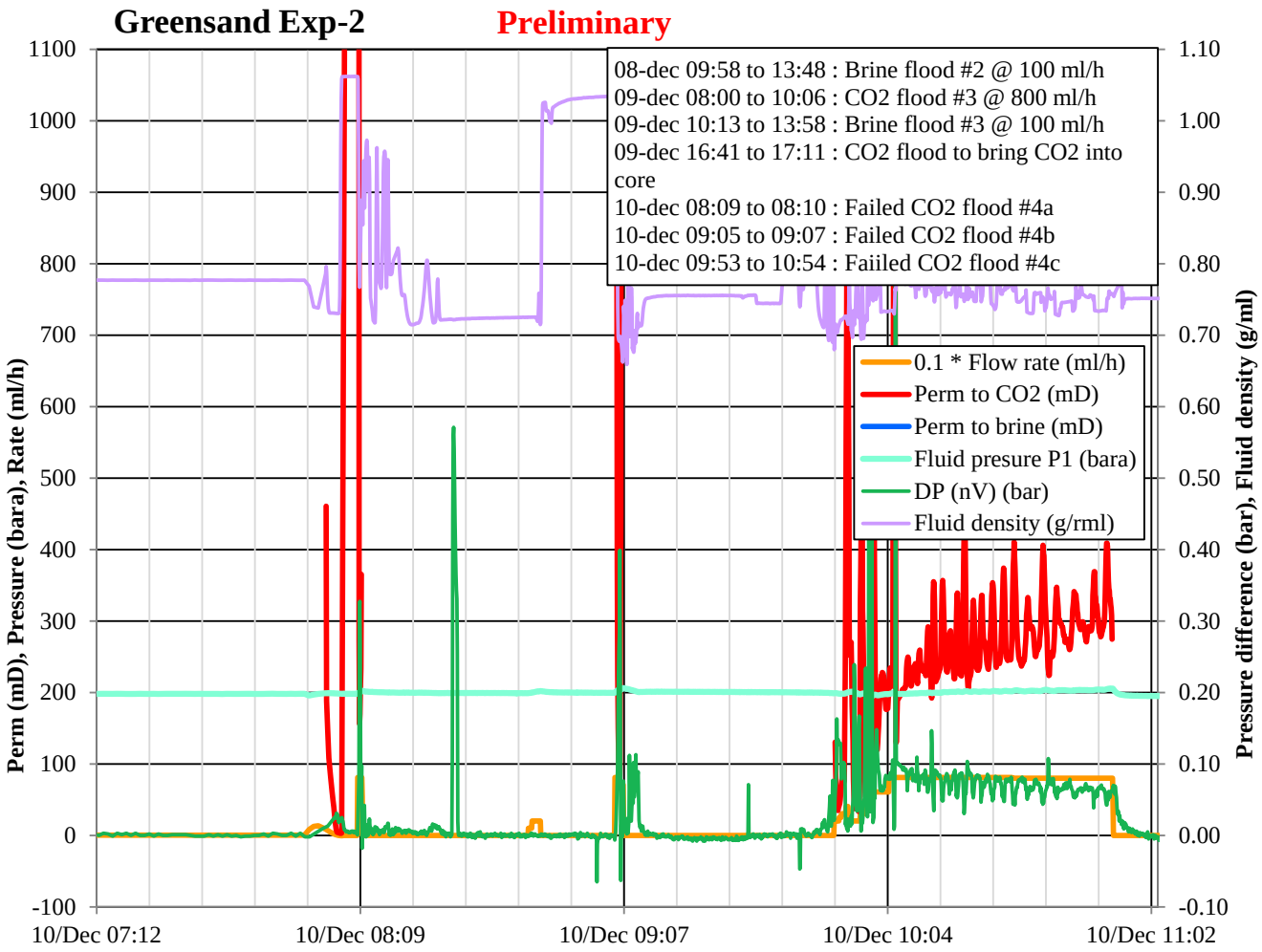

Fig. 15. Experiment Exp-2 failure before CO_2 flow 4.

Fig. 16 shows the last two CO_2 and formation brine injection in Exp-2. In the fourth cycle, the CO_2 was injected for 17 PV's and in the last cycle for 29.79 PV's. The pressure drop across the samples seem to be not constant to reach the stable permeability.

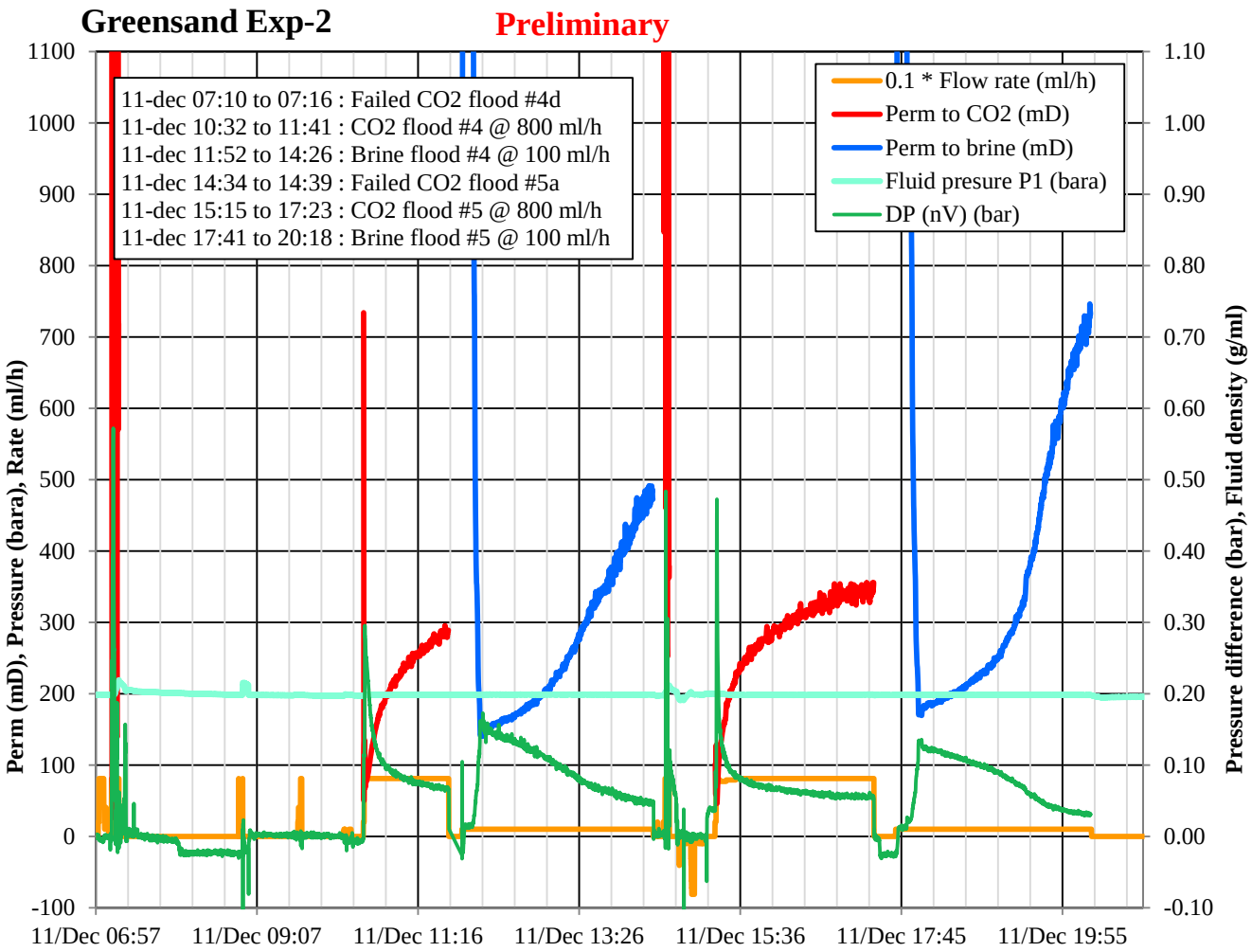

Fig. 16. Experiment Exp-2. Two last CO_2 and formation brine injection.

2.3 Experiment Exp-3

Used material

RRI samples with numbers #100, #101, and #102 were selected for experiment Exp-3. As it shows in Fig. 17, sample #100 was wrapped in a heat shrinkable sleeve and contained filters as received from RRI. The sample was unwrapped before drying and using in Exp-3. Table 6 gives the properties of the core samples. The length of the composite core was 15.05 cm, with pore volume of 59.3 ml and average gas permeability of 1203 mD. The same formation brine as the one used in experiment 1 and 2 was used in Greensand Exp-3. The synthetic brine composition was shown earlier in Table 2.

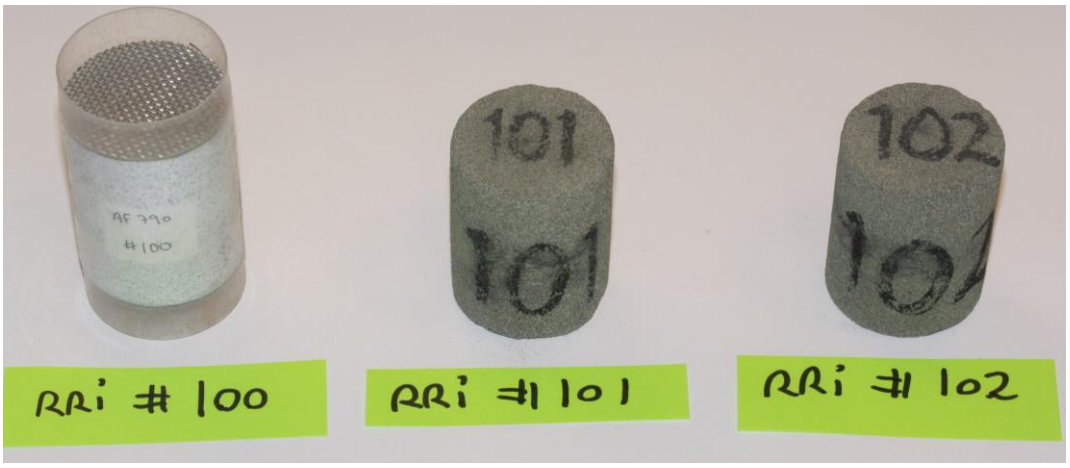

Fig. 17. Plug samples used in experiment Exp-3

Table 6. Exp-3 sample characterization.

Sample Id.			RRI						
	Depth	Orient	Por	Gas perm	Gr. dens.	Diam.	Length	GeomBV	PV
	(MD, m)		(%)	(mD)	(g/ml)	(cm)	(cm)	(ml)	(ml)
100	1778.03	Horiz.	35.4	1140	2.70	3.80	5.03	57.18	20.243
101	1778.32	Horiz.	34.5	1230	2.69	3.77	5.02	56.14	19.369
102	1778.67	Horiz.	34.7	1240	2.69	3.80	5.00	56.81	19.714
Average or cumulative value			34.9	1203	2.69	3.79	15.05	170.14	59.326
Std. dev			0.47	55	0.006	0.16			

Experimental set-up

The three plugs (#100, #101, and #102) were saturated with Nini Formation brine, and were mounted as a composite core sample in a hydrostatic core holder. Two steel filters with 1 mm mesh size were placed at each end of the composite core sample. At this experiment, the rig was modified, and an extra 5 litre cylinder was added to the rig and the pumps were coupled to be able to inject CO_2 at higher flow rates of 1740 ml/h. An additional Vindum Pump was added to the setup in this stage as well. Before starting Exp-3, two experiments to evaluate the pressure drop across the core holder in the tube lines were conducted with mounting the core holder, without any core samples, cf. section "Experimental conditions and procedures".

Fig. 18 shows the restriction at the inlet and the particle trap at the outlet used in Exp-3. The inlet ring has the thickness of 5 mm and the outlet ring has 12.4 mm thickness. The function of these rings at inlet and outlet of the core is different. The inlet ring is a restriction to increase the flow at entrance and the outlet ring is a particle trap, similar to the ones used in both inlet and outlet of Exp-2. The function of this particle trap is to catch the fines early in the flow and prevent any blockage of tube lines. The core holder was mounted in GEUS FC Rig. Two other particle traps were used in the upstream and downstream of the flow stream right before and after the core holder. The core holder in this experiment has horizontal position.

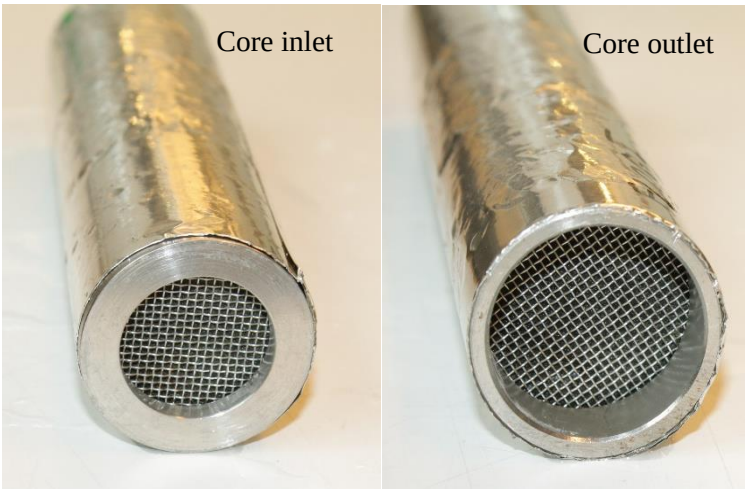

Fig. 18. Exp-3. Appliances used in the core holder in both ends of composite core. Left photo shows the flow restriction with inner diameter of 25 mm.

Flow rate criteria

The information about injection rate at the well surface was reported by INEOS (October 2020) as 10000 m^3/d. A maximum injection fluid velocity of 20 m^3/day/m close to the heel of the wellbore and 10 m^3/day/m at the toe of the wellbore was reported. Considering half of the open hole is cleaned, the reported flow rate is 35.6 ml/min/$inch^2$ close to the heel of wellbore and 17.8 ml/min/$inch^2$ at the toe of the wellbore. Table 7 shows if the flow rate of 27.96 ml/min and 1 inch core plug are used in the experiment, the flow velocity of 20 m3/day/m will be achieved. The flow rate limits for available pumps in the laboratory was 29 ml/min, therefore in agreement with INEOS, it was decided to use a designed ring as restriction of flow in the inlet of the core in Exp-3. The calculations in Table 8 shows that the restriction at the inlet increases the flow per square inch to 2.25 times more than the flow after the entrance section of the core. This can demonstrate the velocity condition of 20 m3/day/m at the heel of wellbore and 10 m3/day/m at the toe of the wellbore in the core scale.

Table 7. The injection velocity and flow rate reported from INEOS for well operation prior Exp-3

INEOS calculations			
condition	Injection (m3/day/m)	Flow rate (ml/min/inch2)	Flow rate for 1/1.5 inch core (ml/min)
Heel of wellbore	20	35.6	27.96/62.9
Toe of wellbore	10	17.8	13.98/31.4

Table 8. The injection rate used in Exp-3 at GEUS core analysis lab

GEUS core analysis lab		
condition	Flow rate (ml/min/inch2)	Flow rate (ml/min)
1 inch surface area (inlet)	36.92	29
1.5 inch core	16.41	29

Reservoir condition experiments

Brine permeability was measured for the core samples at reservoir condition, prior to starting the sequence of CO_2 floodings on March 19th. After brine permeability measurement, CO_2 was injected to fill 50% of the core pore volume on March 22th. At this time, according to the calculations, half of the core contains formation water and half contains CO_2. After 8 days, on March 30th, the high flow CO_2 injection was started at 1740 ml/h (29 ml/min), and later the flow rate was reduced to 800 ml/hr (13.3 ml/min). The flow rate of 1740 ml/h is called high flow rate CO_2 flooding in this report.

The summary of operations for Exp-3 is as follow. CO_2 injection finished after two 5 liter cylinders became empty and brine was injected to check the permeability to brine at the end of CO_2 flooding in this experiment.

1. Mounting core holder with 3 greensand samples in GEUS FC Rig
2. Establishing reservoir conditions
3. Measurement of brine permeability @ 100 ml/h
4. CO_2 injected to fill 50 % of the core pore space, at this stage half of the core is filled with brine and half with CO_2 to increase the contact of two phases in the pore space
5. 8 days pause for further distribution and reaction of brine and CO_2 in the pore space
6. CO_2 flooding from fixed end of core holder towards floating end @ 1740 ml/h, 151 PV's injected in 5.1 hours
7. CO_2 flooding in the same direction @ 800 ml/h, 10.7 PV's injected for 47 minutes
8. Brine flooding in the same direction @ 100 ml/h, 15.4 PV's injected in 9 hours
9. Flooding operation stopped
10. Depressurization and cooling of reservoir rig
11. Dismounting core holder from rig, dismount plug samples from core holder.

Measurement of brine permeability

Permeability to brine was measured by flooding the core samples with Nini Formation brine at 100 ml/h, shown in Fig. 19. Brine permeability for these set of samples are 1050.29 mD and lower than the gas permeability reported by RRI (1203 mD). Brine permeability for these samples were measured two times due to failure occurred in the first attempt. The first permeability measurement was 1013.8 mD and the results is shown in Fig. 20.

Exp-3 was failed once on March 9th after step 4 in the operations summary. The failure started with leaking from pore space through confining medium and the experiment was terminated on March 11th. The reason of this failure was to high extend because of oversized sleeve with iD=38.5 mm. The oversized sleeve was used as it is difficult to mount the core in ordinary sleeve (iD=38.1 mm) with all the extra appliances and easier in oversized sleeve. The experiment restarted again on March 17th and successfully finished on March 31th.

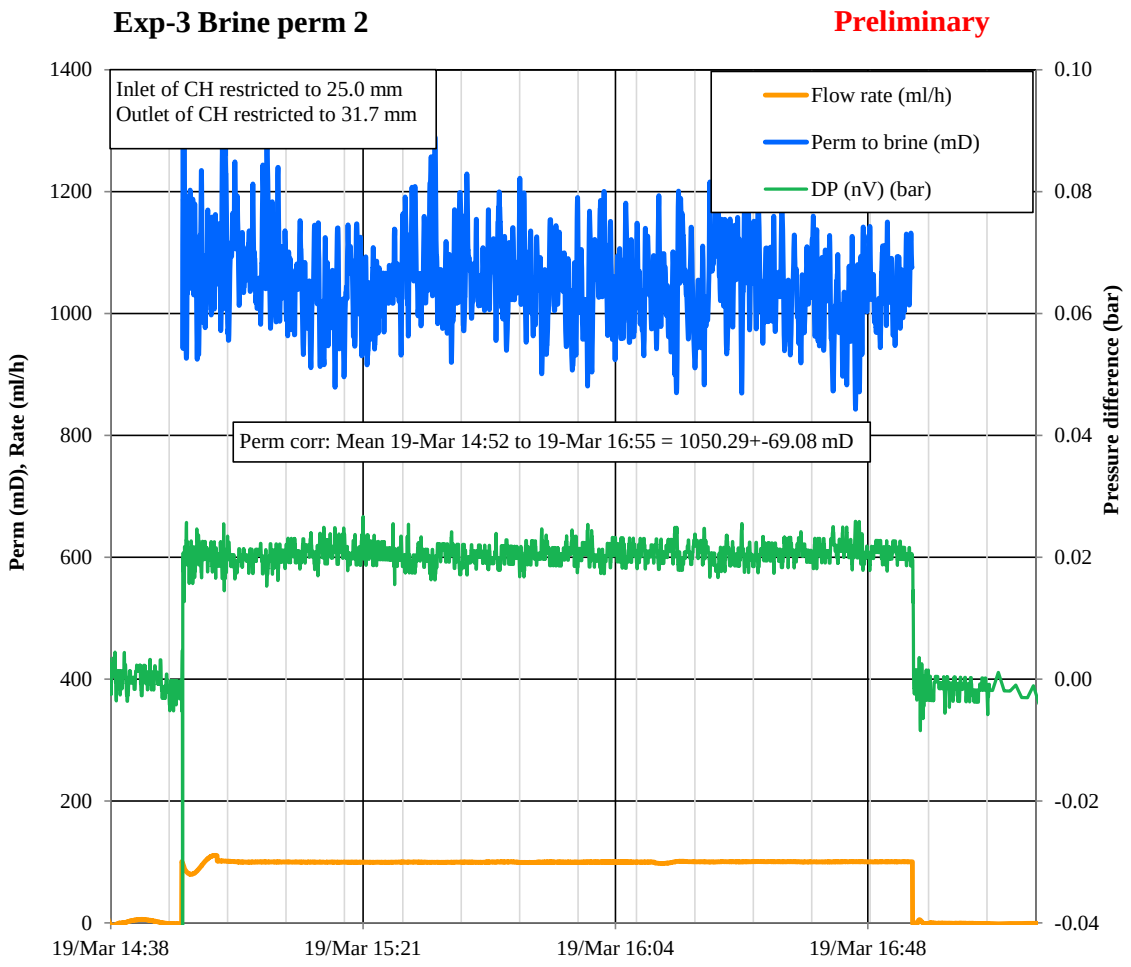

Fig. 19. Experiment Exp-3. Permeability to brine.

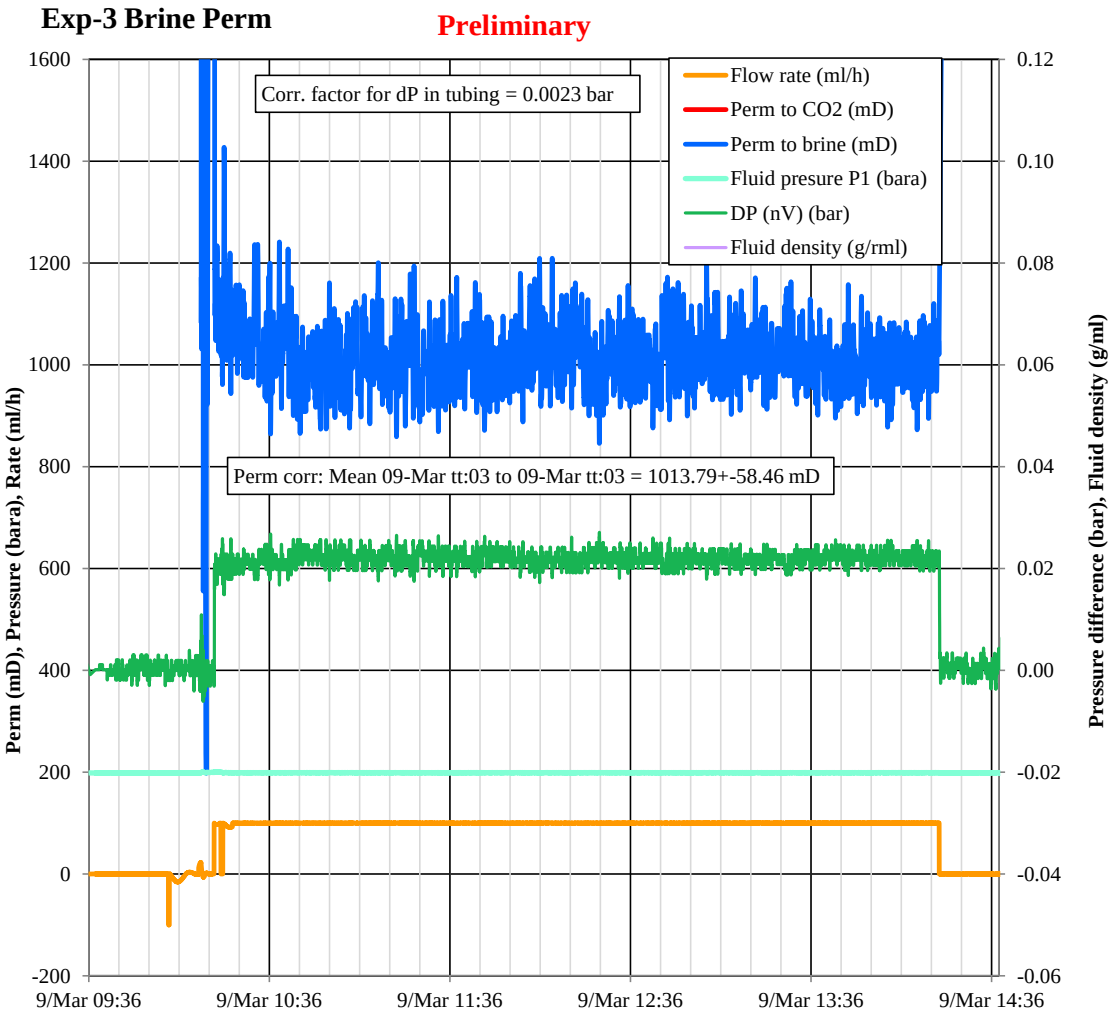

Fig. 20. Permeability to brine in the first attempt to proceed with Exp-3. The experiment was failed after step 4 in the summary of operations.

Overview of flooding operations

CO_2 was injected at two different flow rates in Exp-3 with 1740 ml/h flow rate for 151 pore volumes. The flow rate was decreased without stopping the flow to 800 ml/h. 10.7 pore volumes of CO_2 was injected at this flow rate. After this step, 15.4 pore volumes of Nini formation brine was injected to reach the constant pressure drop across the core sample and permeability to brine was calculated after reaching stable flow. An overview of the flooding sequences is shown versus time and pore volumes in Fig. 21 and 22 respectively.

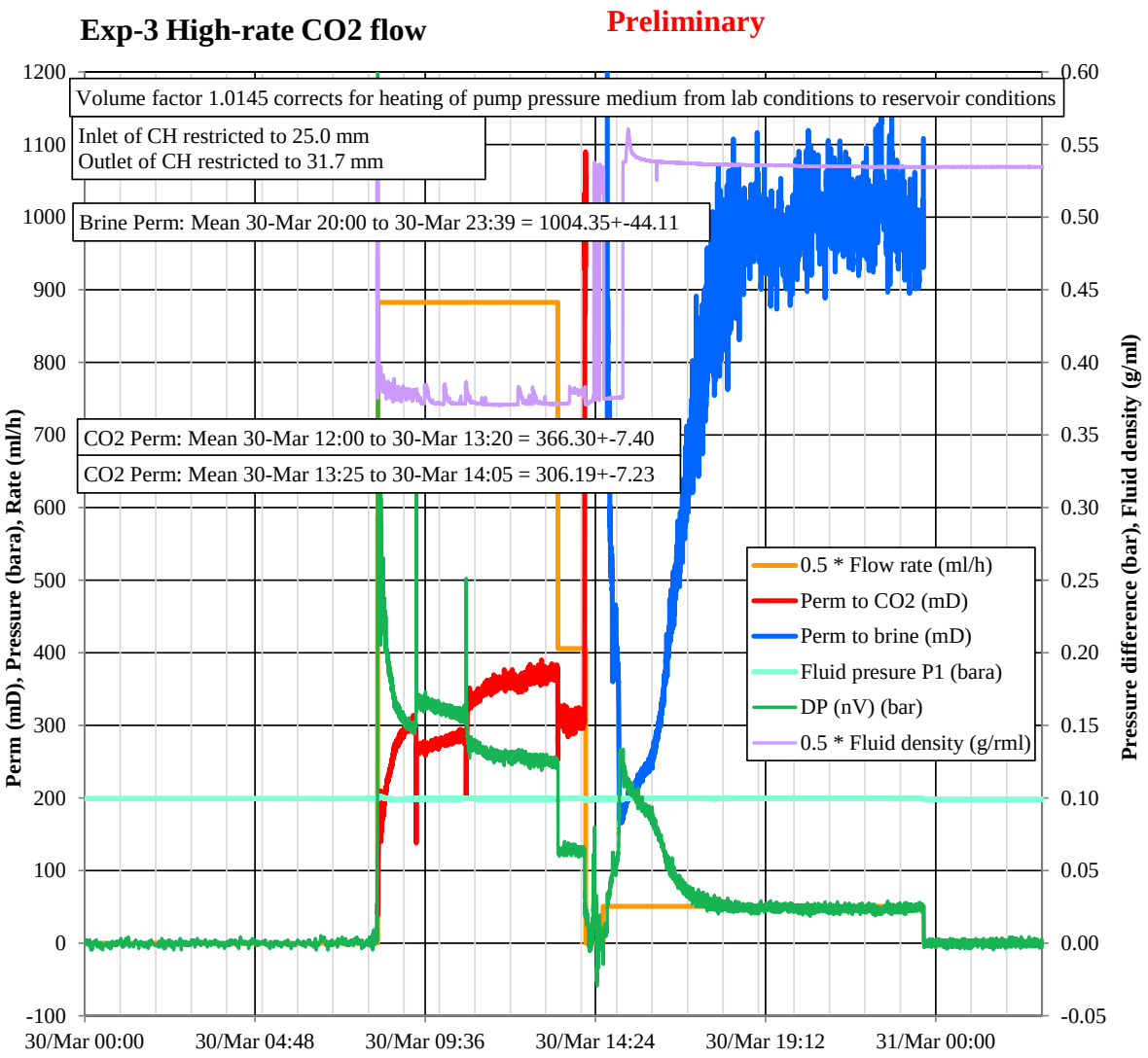

Fig. 21. Experiment Exp-3. High flow rate and low flow rate CO_2 flooding and brine flooding at the end of the experiment.

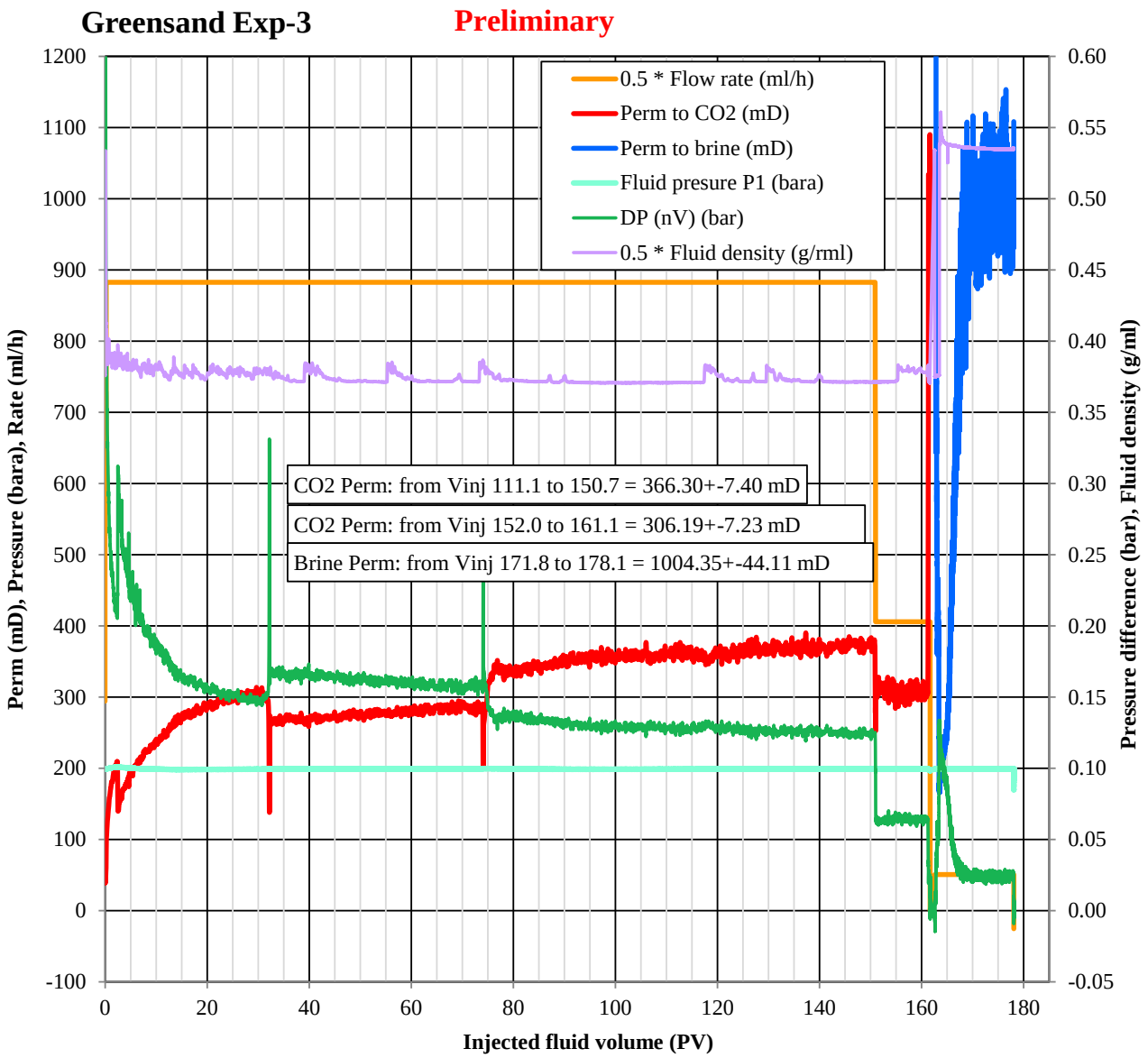

Fig. 22. Experiment Exp-3. Overview of flooding sequences versus injection pore volumes.

Flooding with CO_2 at two flow rates

At the start of the high flow rate CO_2 flooding, a drop in injectivity occurred 5 minutes after starting the experiment. At this time, 2.44 pore volumes of CO_2 were injected at 1740 ml/h. This instance is shown in detail in Fig. 23. The reason for this drop is discussed in the Discussion section.

After 65 minutes at PV=32.2 from starting CO_2 injection, a drop in injectivity has occurred without any operation during flooding experiment (Fig. 24). This drop got resolved after 41.6 pore volumes at PV=73.8 when an operational action occurred (shown in Fig. 25).

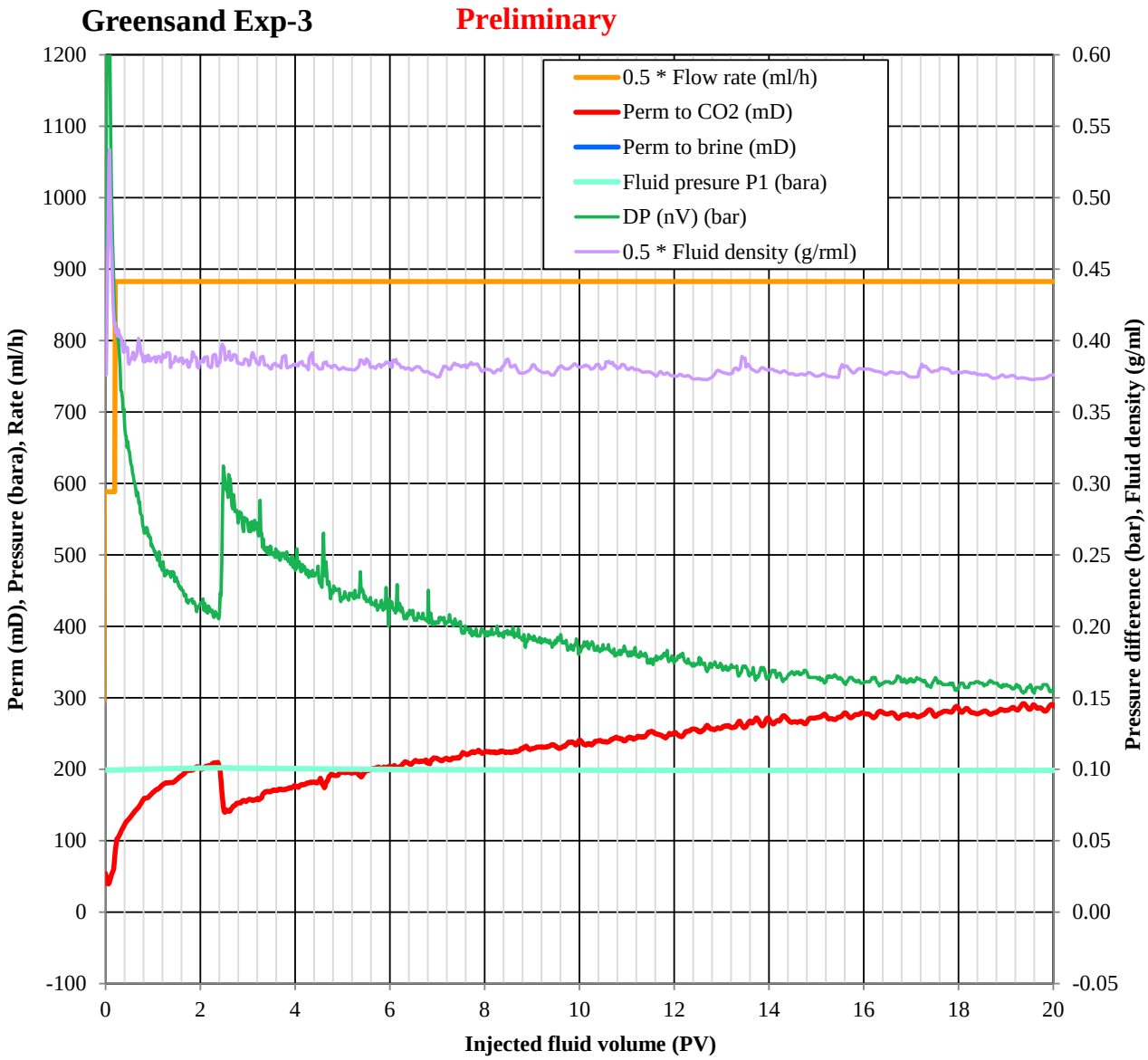

Fig. 23. Experiment Exp-3. The first drop in injectivity of CO_2 early at the beginning of CO_2 flooding.

At PV= 73.8, a valve to the pressure cylinder GAS (CO_2) outlet opened to use the CO_2 from this cylinder. Opening this valve, added 0.7 bar to the pressure fluid of both inlet and outlet of the core samples. The reason of this shift in the injectivity and healing by having a pressure increase of 0.7 bar is not clear. It can be an indication of two flow paths that CO_2 could shift between them.

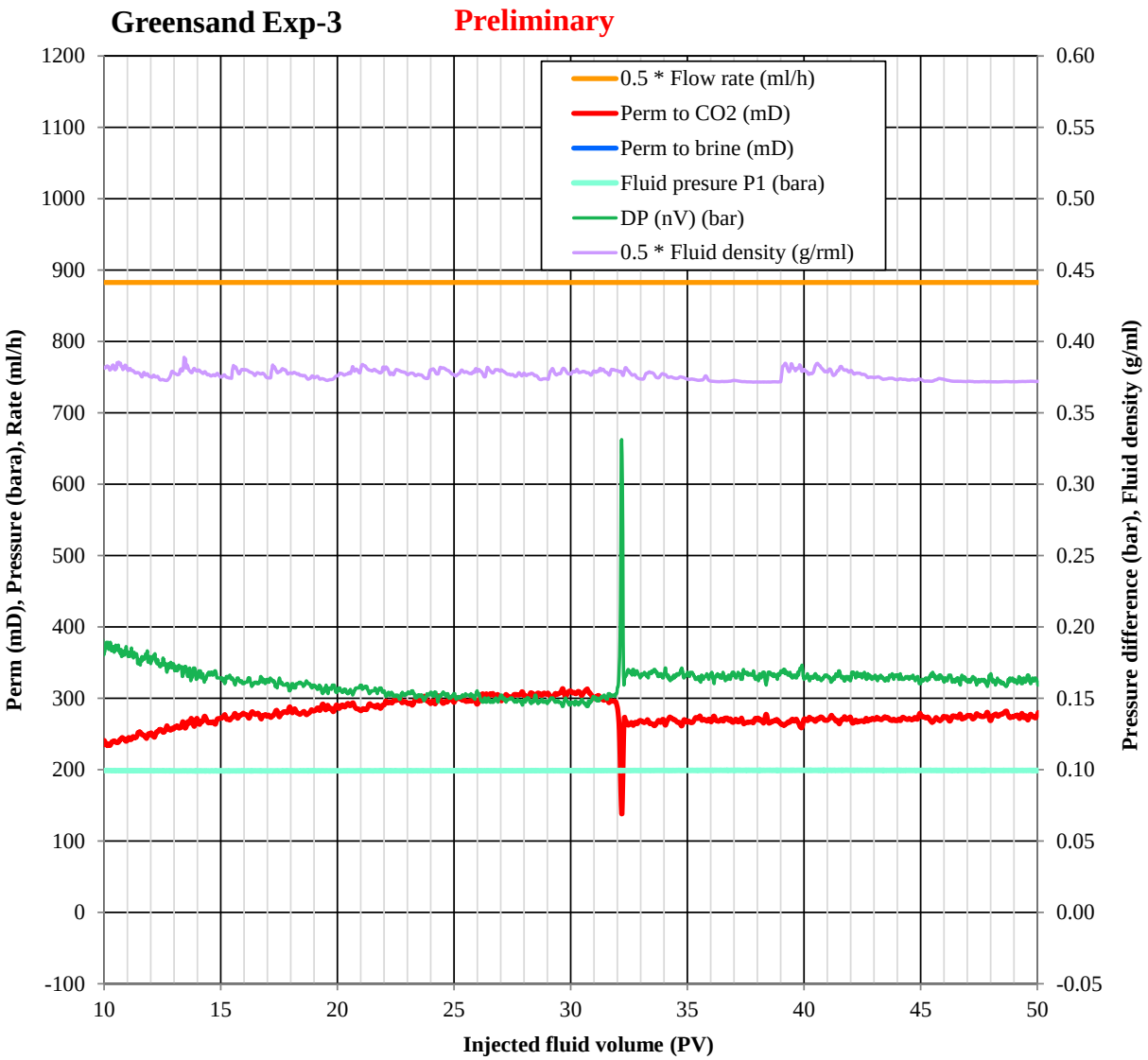

Fig. 24. Experiment Exp-3. The drop in injectivity at 32.2 PV's of injection which was resolved at PV=73.8.

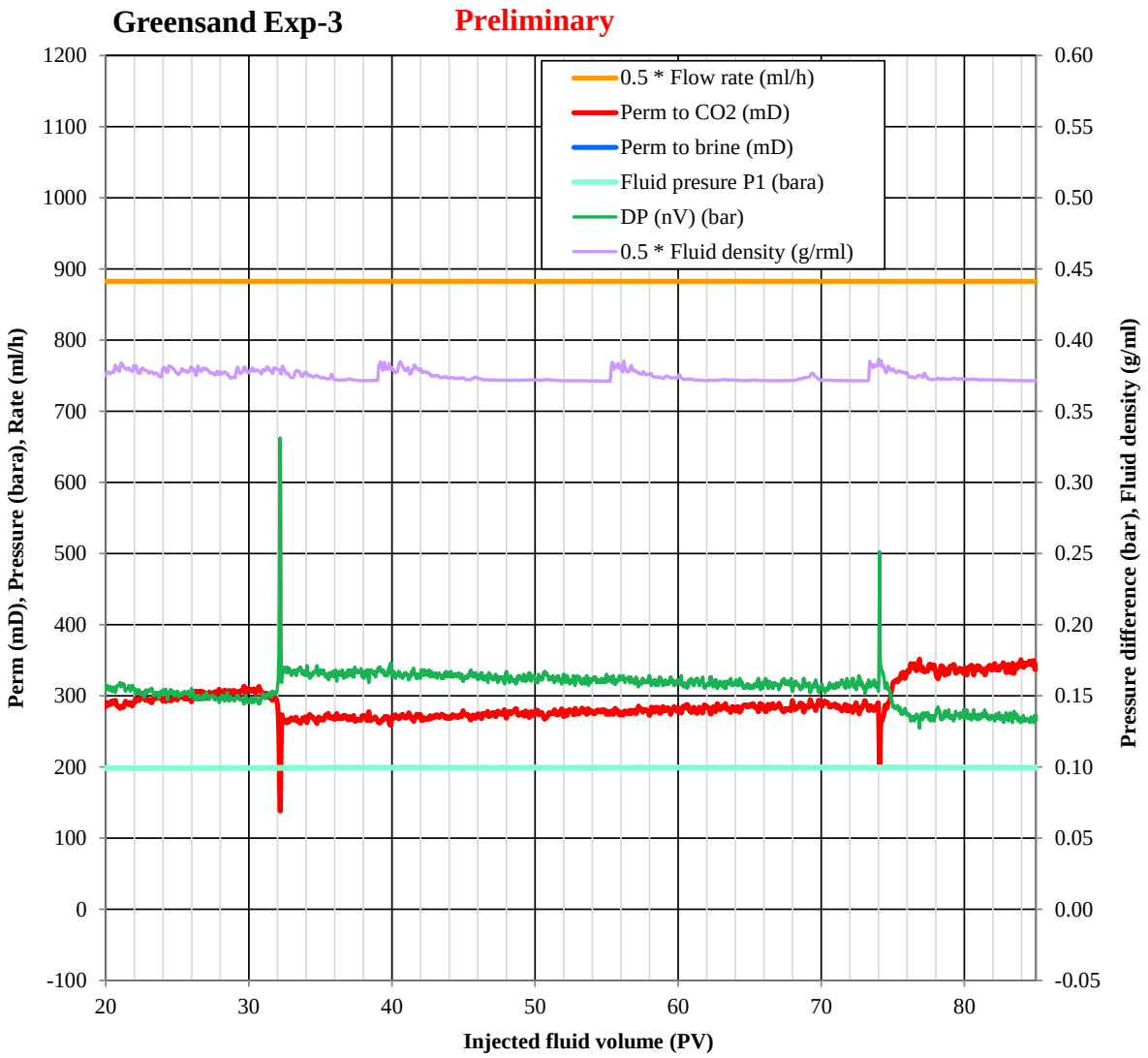

Fig. 25. Experiment Exp-3. The healing of injectivity at PV=73.8 to the continuation of the same level as before dropping at PV=32.2.

Flooding with brine at the end

After injecting 161.7 PV's of CO_2, formation brine was injected to evaluate any changes to brine permeability. The calculated brine permeability is 1004.35 mD after stable flow through the core which is not different from the brine permeability prior starting CO_2 injection (1050.29 and 1013.79 mD). Permeability curve related to second brine flooding is shown in Fig. 26. The ΔP increases when brine starts displacing CO_2 and after 0.89 PV, reduced slowly until it gets stable. It took 7.3 PV's for the brine to reach the stable flow through the core.

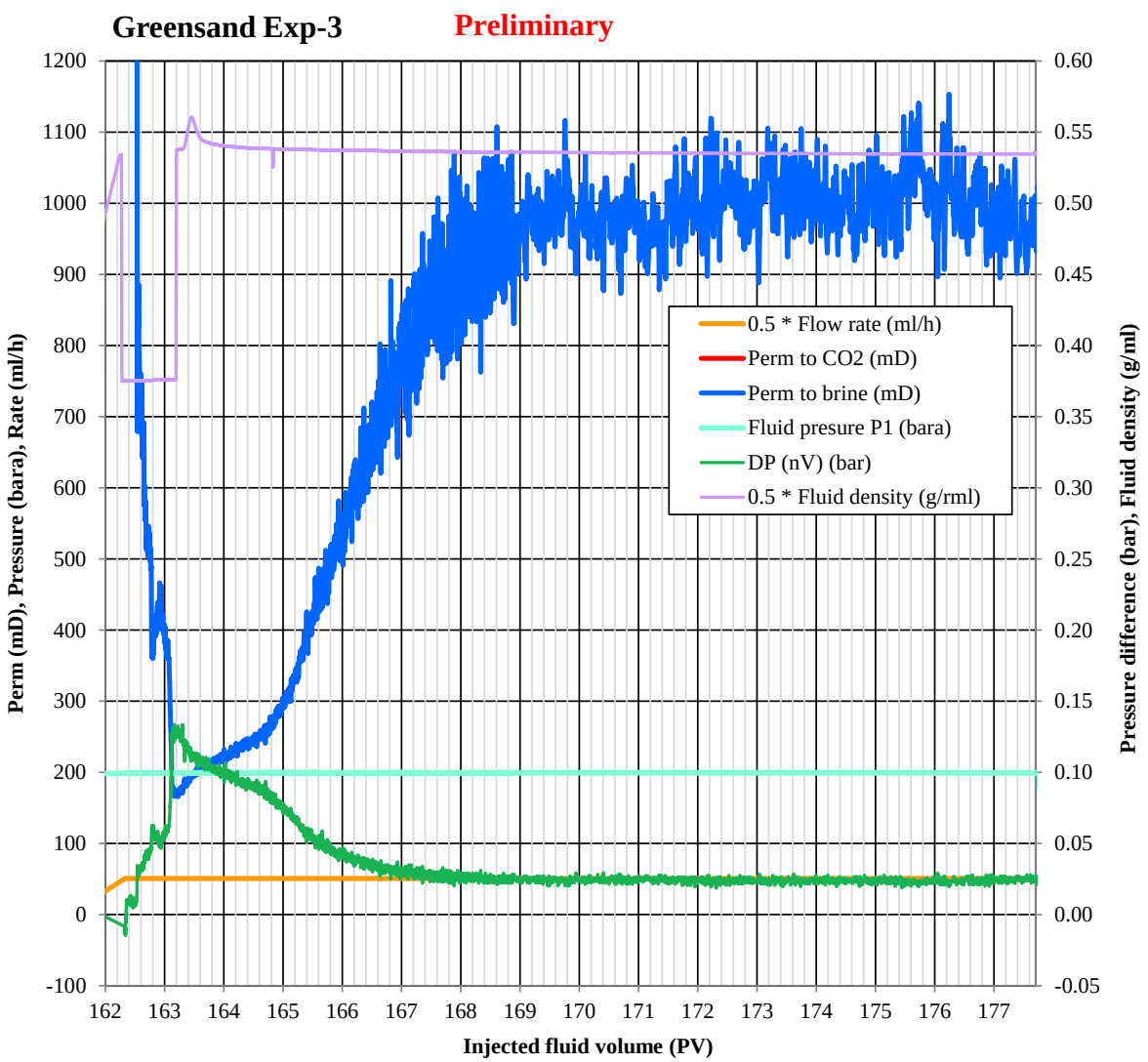

Fig. 26. Experiment Exp-3. Second brine flooding after CO_2 injection.

2.4 Experiment Exp-4

Exp-4 was conducted to verify the injectivity results of the previous experiments, and to obtain information of the water saturation of the core samples at the end of a CO_2 flooding. Exp-4 is different from Exp-3 in the case that in Exp-4, the high flow rate CO_2 flooding was injected in the first cycle, with the core with water saturation Sw=100%, but the initial water saturation of core samples was reduced to 50% before high flow rate CO_2 flooding in Exp-3.

RRI samples with numbers #86, #87, and #108 were selected for experiment Exp-4 (Fig. 27). The handling of the samples by RRI is described in "Experimental conditions and procedures" section. The sample preparation for Exp-4 consisted of (1) saturating the samples with FW, and (2) checking the fluid saturation with an Archimedes determination. Table 9 gives characteristics of the core samples.

Fig. 27. Plug samples used in experiment Exp-1, 86, 87, and 108.

Table 9. Exp-4 sample characterization.

Sample Id.			RRI			GEUS			
	Depth	Orient	Por	Gas perm	Gr. dens.	Diam.	Length	GeomBV	PV
	(MD, m)		(%)	(mD)	(g/ml)	(cm)	(cm)	(ml)	(ml)
86	1773.33	Horiz.	35.0	1590	2.69	3.76	4.96	55.02	19.26
87	1773.65	Horiz.	34.8	1580	2.69	3.76	4.96	55.18	19.20
108	1780.65	Horiz.	34.1	1240	2.68	3.80	4.48	50.85	17.34
Average or cumulate value			34.6	1470	2.687	3.77	14.4	161.05	55.80
Std. dev			0.5	200	0.006	0.02			

Experimental set-up

The three plugs (#86, #87, and #108) were saturated to Sw=100% with Nini Formation brine (Table 2) and were mounted as a composite core sample in a hydrostatic core holder. Upon mounting the core samples in the core holder, (1) steel filters with 1 mm mesh size were mounted at each end of the composite core sample, (2) a flow restriction with inner diameter of 25 mm was installed upstream to the core samples, (3) a particle trap with inner diameter of 32 mm was installed downstream to the core samples, and (4) the whole core assembly was wrapped in tin foil prior mounting in the sleeve. Fig. 28 shows the items of the core assembly. The core holder was mounted in a horizontal position in the FC Rig. This experimental set-up is identical to Exp-3.

Fig. 28. Core assembly for Exp-4. Items comprising the core assembly are shown sequentially from inlet to outlet of the core holder, with inlet at the right and outlet at the left. Rightmost is the inlet aperture with inner diameter 25 mm, leftmost is the particle trap with inner diameter 32 mm. Adjacent to the core samples are the two filters with 1 mm mesh size.

Reservoir condition experiments

The experimental conditions for Exp-4 are summarized in Table 1, which are identical to Exp-2 and Exp-3.

Summary of operations during core flooding Exp-4:

1. Mounting core holder in horizontal position with 3 greensand samples in GEUS FC Rig.
2. Establishing reservoir conditions, 200 bara, 60 °C.
3. Brine permeability measurement: Flooding with Nini formation water @ 100 ml/h, 4.2 PV's injected in 4.2 hours.
4. 1st CO_2 flooding: Flooding with CO_2 @ 1740 ml/h, 73.0 PV's injected in 2.3 hours, followed by flooding with CO_2 @ 800 ml/h, with 15.9 PV's injected in 1.1 hour.
5. 1nd Brine flooding: Flooding with Nini formation brine @ 100 ml/h, 9.3 PV's injected in 5.0 hours.
6. Injection of CO_2 to fill 50% of the pore space of the core sample.
7. No-flow condition for 5 days 22 hours at reservoir conditions
8. 2nd CO_2 flooding: Flooding with CO_2@ 1740 ml/h, 72.8 PV's injected in 2.3 hours, followed by flooding with CO_2 @ 800 ml/h, with 13.5 PV's injected in 0.9 hour.
9. Depressurization and cooling of reservoir rig
10. Dismounting core holder from rig, dismount plug samples from core holder, core samples analysed for water saturation by Dean Stark extraction
11. Collection of samples of particles from the four particle traps of the rig.

Fig. 29 gives an overview of the flooding operations in Exp-4.

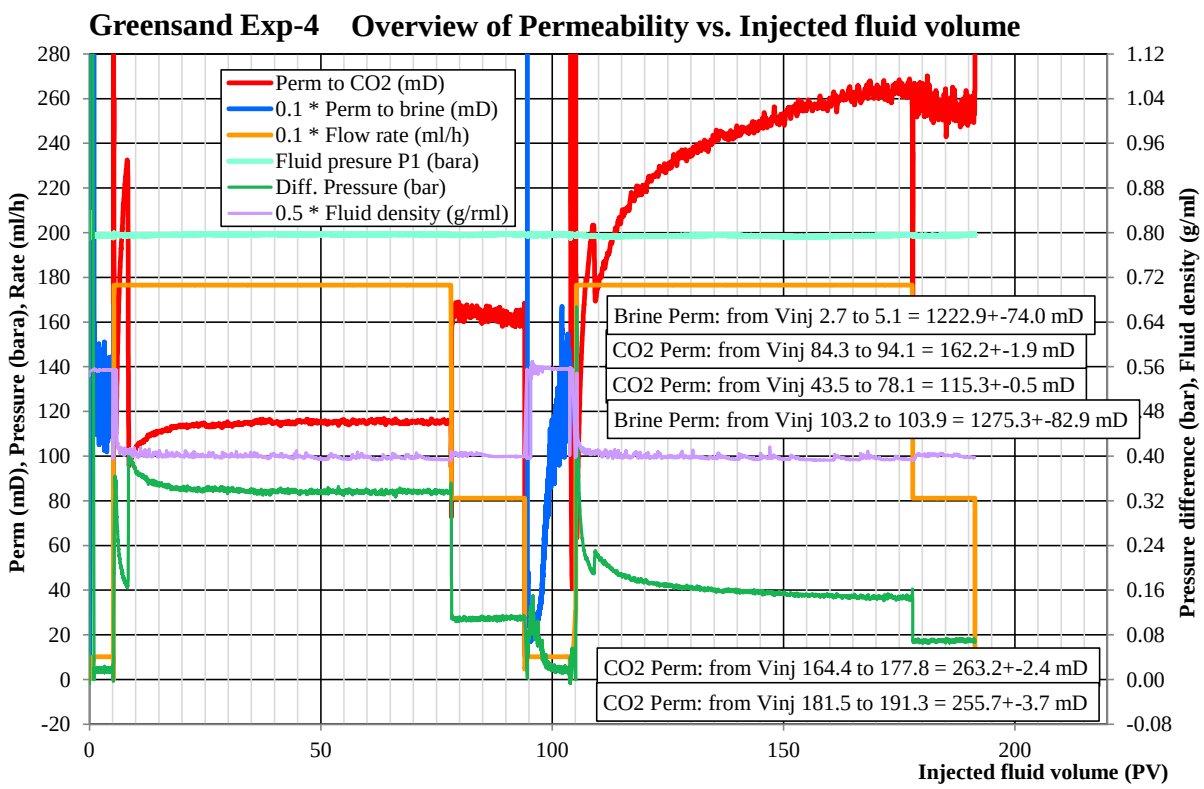

Fig. 29. Overview of Exp-4. The brine permeability is divided to 10 to be able to be shown in the figure.

During Exp-4 the densitometer of the FC Rig did not function as it should. In two periods with flow of pure Nini formation brine the density measurements were determined to be 0.06 g/ml too high, and similarly the density measurements were determined to be 0.07 g/ml too high during one period with flow of pure CO_2. Apart from this, the densitometer apparently worked as it should, in particular the fluid changes from brine to CO_2 and vice versa are consistently recorded. The densitometer problem resembles the problem experienced during Exp-3, where it was caused by precipitation of solid material from the fluid flow inside the densitometer measuring cell.

Brine permeability measurement

Initial permeability to brine was measured by flooding the core samples with Nini Formation brine at 100 ml/h, cf. Fig. 30. A total of 4.2 PV's of brine were injected in 2.3 hours. A brine permeability of 1223 mD was measured. The mean value of the 3 gas permeability determinations of RRI is 1470 mD (Table 9).

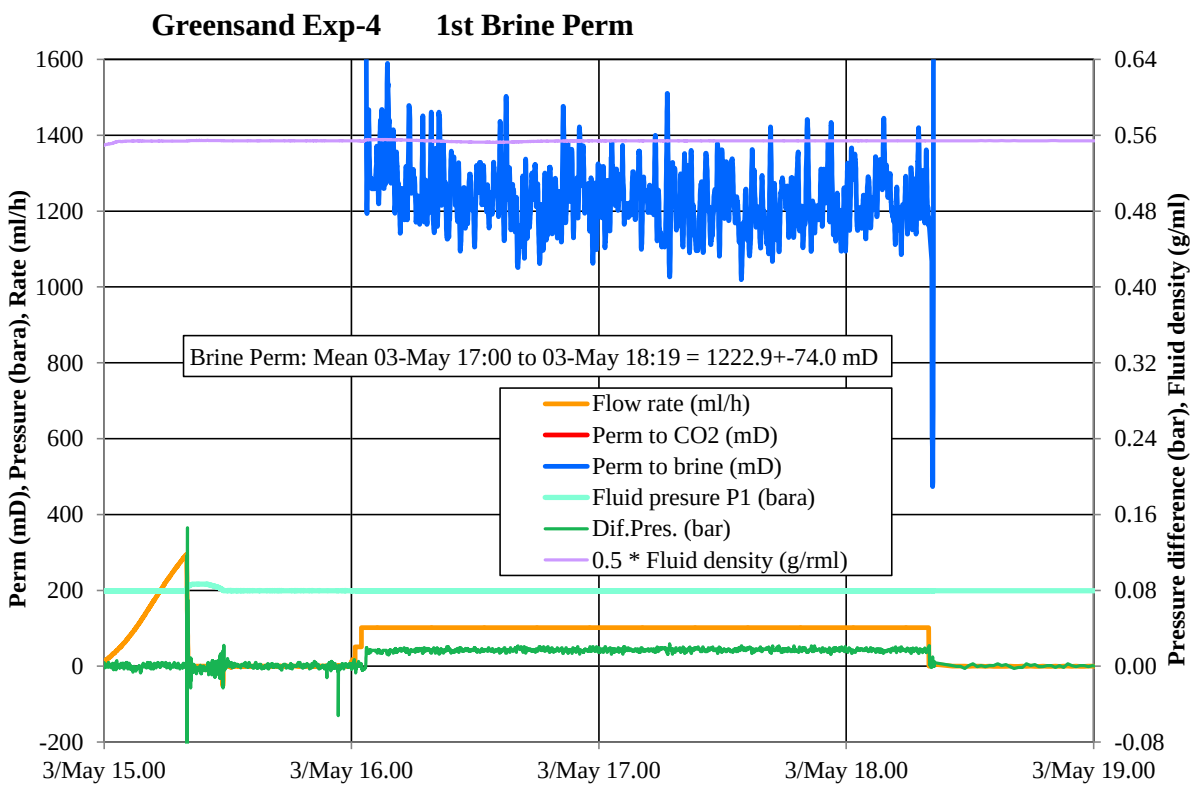

Fig. 30. Experiment Exp-4. First brine flooding at 100 ml/h.

First flooding with CO_2

Fig. 31 shows a diagram of the first CO_2 flooding of Exp-4. A high-rate flooding at 1740 ml/h lasted 2.3 hours with an injected volume of 73.0 PV's of CO_2. Without stopping the flow, the injection was followed by a low-rate flooding at 800 ml/h where 15.9 PV's of CO_2 were injected in 1.08 hours.

At the start of the flooding, the pore space of the core sample was saturated with formation water, i.e. it did not contain any CO_2. Breakthrough of CO_2 occurred after injection of 0.6 PV of CO_2. The permeability log starts with a steep rise from approximately 110 mD to 232 mD, which is reached after 6 minutes of flow equal to 3.0 PV's of injected CO_2. At this point, the permeability log makes a pronounced change and drops steeply to 96 mD, which is reached 42 seconds after the permeability peak at 232 mD. The permeability then slowly recovers to 115 mD, which is reached 60 minutes after start of the flooding, equal to 32 PV's of injected CO_2. During the last half of the high-rate CO_2 flooding the permeability does not change but remains stable at 115 mD. Fig. 32 shows a diagram of the initial part of the first CO_2 flooding of Exp-4.

At the end of the high-rate CO_2 flooding, the flow rate was reduced to 800 ml/h. The permeability immediately increased to between 160 mD and 165 mD, where it remained with minor variation for the rest of the low-rate flooding. A total of 88.9 PV's of CO_2 were injected during the combined high-rate ad low-rate CO_2 floodings (Fig. 29).

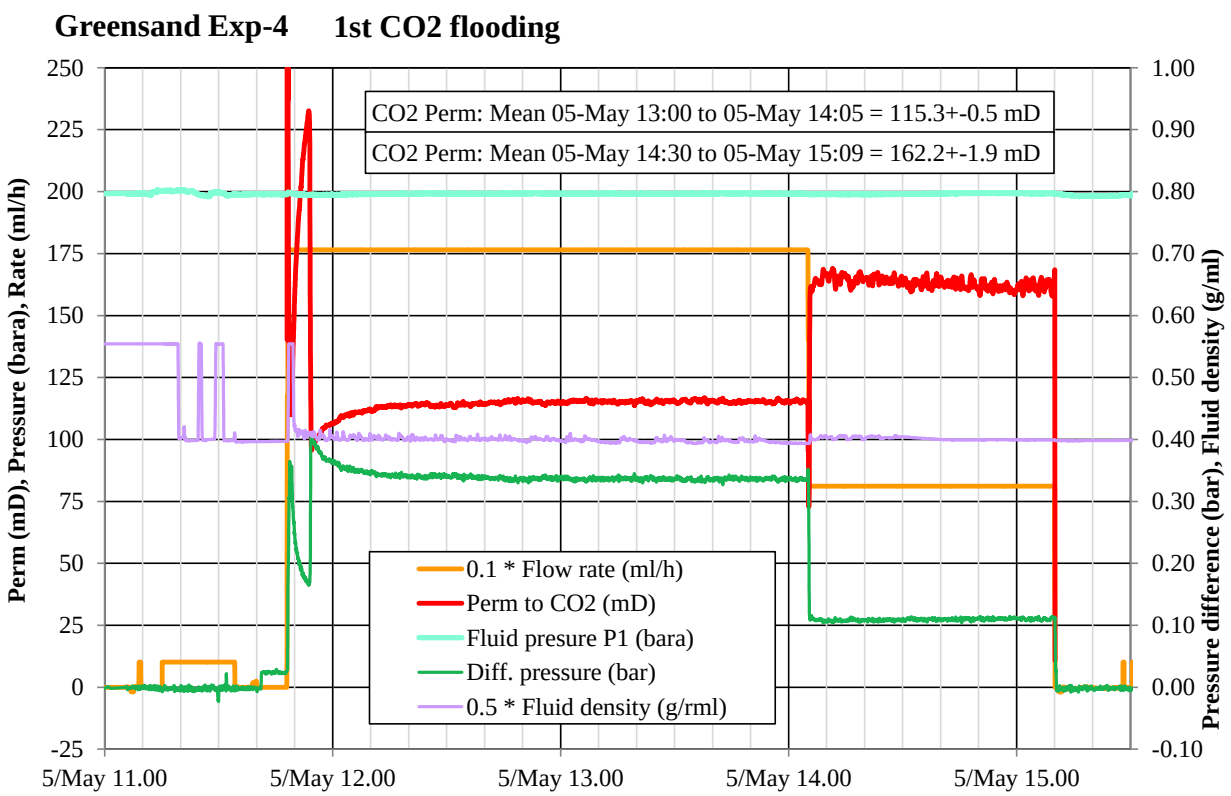

Fig. 31. Experiment Exp-4. First CO_2 flooding.

As it shows in Fig. 32, the breakthrough of CO_2 occurred after injection of 0.6 PV. After CO_2 breakthrough the fluid density trace shows a distinctly fluctuating trend that indicates the production of water carried by the supercritical CO_2, either as a moving film on the walls of the rig tubing or as discrete droplets suspended in CO_2.

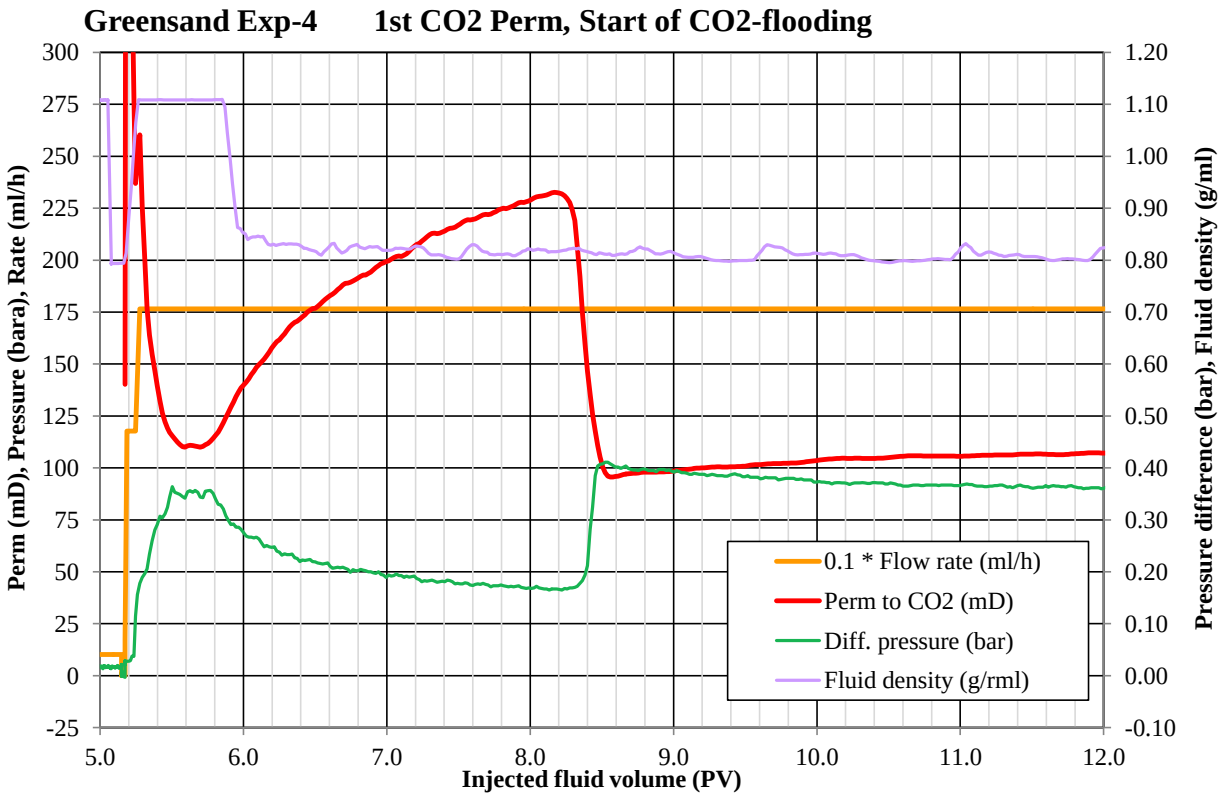

Fig. 32. Experiment Exp-4. Start of first CO_2 flooding.

Brine flooding between two CO_2 floods

Permeability to Nini Formation brine was measured for the second time with start of the flooding 38 minutes after the end of the first CO_2 flooding at 800 ml/h. A log of the flooding is given in Fig. 33. The brine flow rate was 100 ml/h, and the PT conditions were the same as in the first brine flooding, i.e. 200 bara and 60 °C. A difference from the first brine flooding was that at the start of the second brine flooding the core sample contained a significant saturation of supercritical CO_2.

A total of 9.3 PV's of brine were injected at 100 ml/h in 2.3 hours. Water breakthrough occurred after injection of 0.84 PV's of brine. After that the permeability to brine increased steadily and reached 1275 mD at the end of the flooding. This is within uncertainty the same as the permeability of 1223 mD measured at the end of the first brine flooding. It also agrees with the mean gas permeability determination of RRI at 1470 mD (Table 9).

The permeability to brine was not completely stable at the end of the second brine flooding, and a minor increase in brine permeability would probably have occurred if the flooding had continued. The flooding was stopped because of limited brine supply.

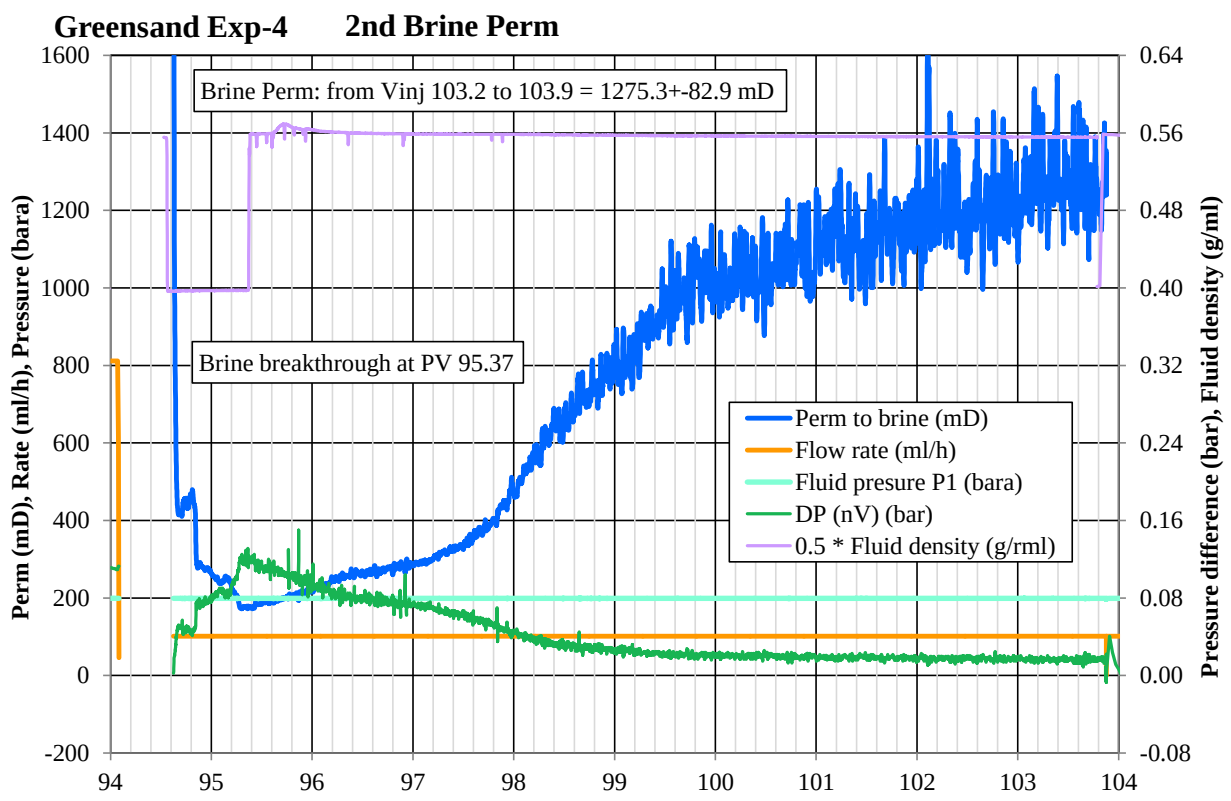

Fig. 33. Experiment Exp-4. Second brine flooding at 100 ml/h.

Second flooding with CO_2

13 hours after the first brine flooding, approximately 27 ml of CO_2 was injected into the pore space of the core sample. The volume was calculated to obtain a mean CO_2 saturation of 50% in the pore space. The core samples then rested for 5 days and 22 hours at reservoir conditions without any flow to allow chemical reactions between the fluids and the matrix grains of the core sample. After that the second CO_2 flooding was conducted.

Fig. 34 shows a diagram of the second CO_2 flooding of Exp-4. A high-rate flooding at 1740 ml/h lasted 2.3 hours with an injected volume of 72.8 PV's of CO_2. Without stopping the flow, the injection was followed by a low-rate flooding at 800 ml/h where 13.5 PV's of CO_2 were injected in 0.92 hours. At the start of the second CO_2 flooding, the pore space of the core sample contained a mixture of brine and supercritical CO_2. The permeability log (Fig. 34) starts with a steep rise from approximately 70 mD to 203 mD, which is reached after 7 minutes of flow equal to 3.8 PV's of injected CO_2. At this point the permeability log makes a pronounced change and drops steeply to 169 mD, which is reached 36 seconds after the permeability peak at 203 mD. The permeability then increases again to reach 263 mD, 2.3 hours after start of the flooding. During the final 0.3 hours of the flooding the permeability was stable.

At the end of the high-rate CO_2 flooding, the flow rate was reduced to 800 ml/h. The permeability did not change significantly, but reduced slightly to 255.7 mD. A total of 86.2 PV's of CO_2 were injected during the combined high-rate ad low-rate CO_2 floodings (Fig. 29).

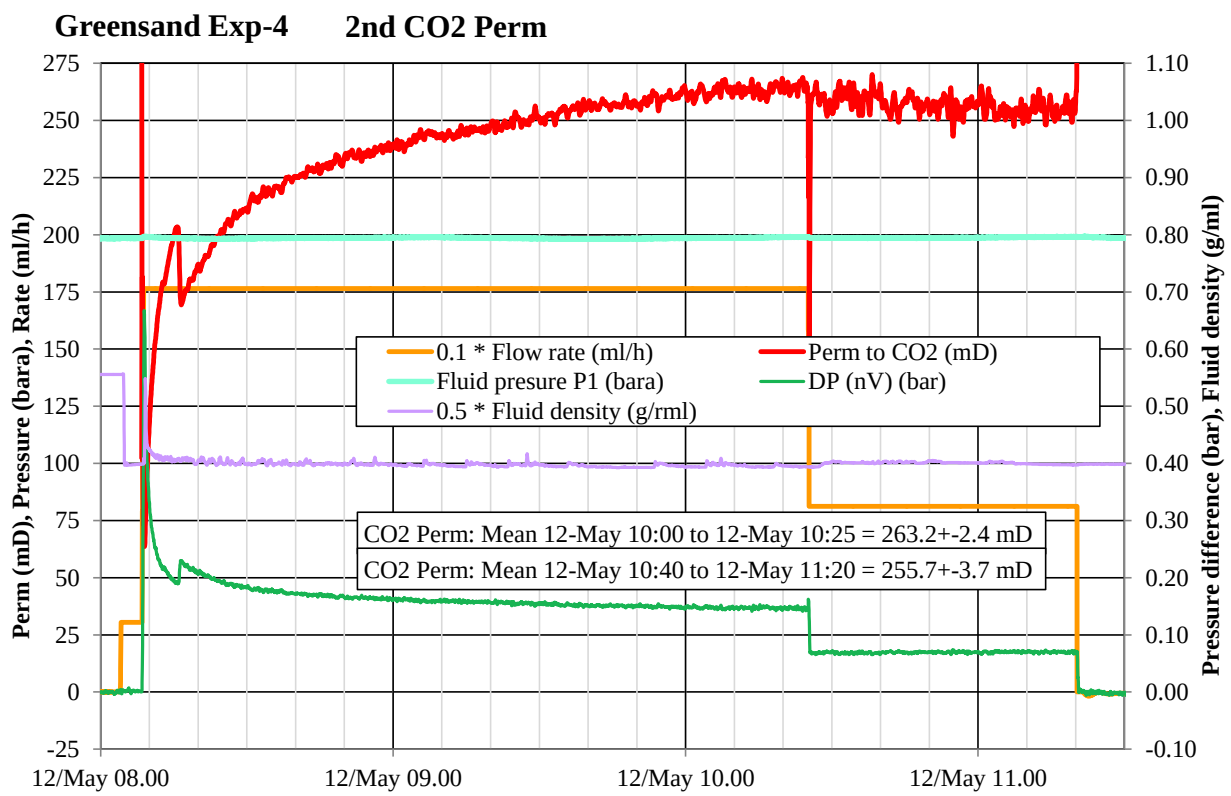

Fig. 34. Experiment Exp-4. Second CO_2 flooding.

Fig. 35 shows a diagram of the initial part of the second CO_2 flooding of Exp-4. The permeability log starts with a steep rise from approximately 70 mD to 203 mD, which is reached after 3.8 PV's of injected CO_2. At this point the permeability trace makes a pronounced change and drops steeply to 169 mD, which is reached after injection of a further 0.3 PV's of CO_2. The permeability then recovers steadily to 263 mD, which is reached after injection of approximately 73 PV's of CO_2.

At the start of the second CO_2 flooding, water was produced for a few seconds, followed by breakthrough of CO_2. This shows that nearly all of the core sample contained a mixture of brine and CO_2 during the 6-day equilibration before the second CO_2 flooding. After CO_2 breakthrough the fluid density trace shows a distinctly fluctuating trend that indicates the production of water carried by the supercritical CO_2, either as a moving film on the walls of the rig tubing or as discrete droplets suspended in CO_2.

The drop in permeability in the second CO_2 flooding is smaller than the drop in the first CO_2 flooding (Fig. 29), but otherwise the log pattern is similar.

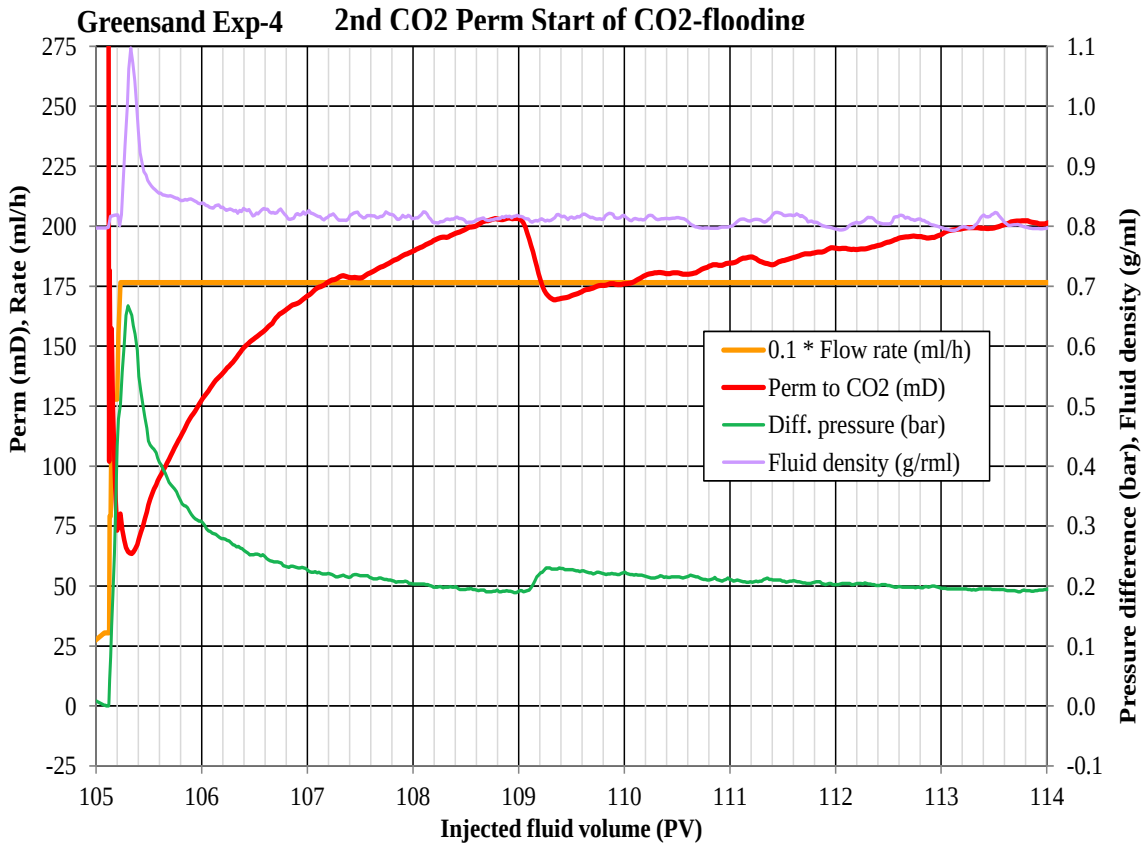

Fig. 35. Experiment Exp-4. Start of second CO_2 flooding.

Water saturation data

After depressurization and cooling of the rig the core samples were dismounted from the core holder. The core samples proceeded to Dean Stark extraction to determine their water saturation. During unloading of the samples from the core holder care was taken to avoid contamination of the samples with water from the core holder annulus. The results of the Dean Stark extraction are given in Fig. 36, where the measured water saturation values are plotted against the distance of the sample centre from the core inlet.

The measured water saturation values are considered to represent the water saturation of the core samples at reservoir conditions, at the end of the second CO_2-flooding of Exp-4, except that some water may possibly have been lost from core samples by expulsion of expanding CO_2 during depressurization of the experiment. However, it is not considered likely that more than relatively small amounts of water were lost, because the core holder inlet was closed during depressurization. Therefore, only the CO_2 volume present in the core holder, approximately 0.55 PV, was depressurized from the core holder. This amount of CO_2 can only dissolve a limited amount of water.

Fig. 36 shows that a strong gradient in water saturation existed at the end of the second CO_2-flooding of Exp-4. Sample 86, which formed the inlet end of the composite core sample, had a water saturation of 28.3%. Sample 87, which formed the middle of the composite core sample, has a water saturation of 40.5%. Sample 108, which formed the outlet end of the composite core sample, had a water saturation of 65.3%.

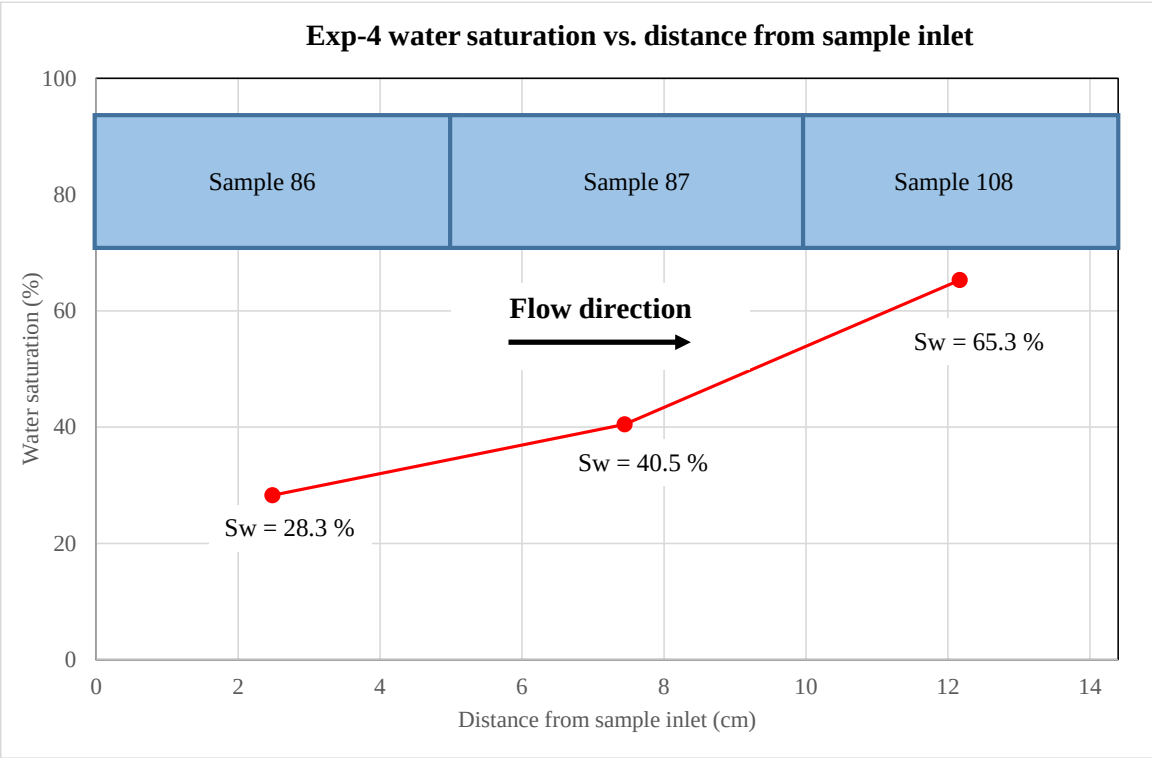

Fig. 36. Experiment Exp-4. Water saturation vs. distance from inlet of core sample.

3. Discussion

The experimental plan for the four experiments had a common frame using composite cores comprised of three 1.5” subsamples with total length approximately 15 cm. All experiments were conducted at fluid pressure 200 bara and temperature 60 °C. Reservoir fluids were commercial CO_2 purity 4.0 and synthetic Nini formation water. Flooding rates were 100 ml/h for brine and 800 and 1740 ml/h for CO_2. These common conditions make the experiments highly comparable. Some conditions were however modified between experiments. These modifications include:

1) After Exp-1, particle traps were installed inside the core holder at both core ends. After Exp-2, Exp-3, and Exp-4 these traps contained significant amounts of fines, typically 0.1 to 0.3 grams. The particle traps had inner diameter of 32 mm, and thus reduced the effective cross section for flow from 38 mm to 32 mm.
2) In all 4 experiments, two particle traps were installed outside the core holder, one 18 cm upstream to the core holder, and one 42 cm downstream to the core holder. The upstream trap never contained significant amounts of fines, but after Exp-2, Exp-3, and Exp-4, the downstream trap did contain resp. 0.0289 g, 0.010 g and 0.008 g of fines that had travelled the 42 cm from the core sample through the tubing of the rig. These fines are currently being investigated.
3) The core orientation was changed from vertical to horizontal after Exp-1.
4) A constriction with inner diameter of 25 mm was installed at the core inlet after Exp-2, which reduced the effective cross section for flow at the inlet from 38 mm to 25 mm. This was requested by INEOS and Wintershall DEA to increase the fluid velocity at the core inlet.
5) The set-up of flooding periods with brine and CO_2 differed between the four experiments. Details are given below and in the description of each experiment.

Table 10 gives a summary of the 14 brine-flooding operations of the four experiments. Permeability to brine was measured at the start of each experiment at Sw =100%, Figs. 4, 12, 19, and 30. These measurements are identified as "Initial Brine" permeability. A stable permeability measurement was obtained for all four experiments with a brine permeability value that fell in the range between 79% and 87% of the gas permeability value reported in the core analysis report from RRI.

In Exp-1 permeability to brine was measured after each of the two CO_2 flooding operations (Fig. 6), and in Exp-2 permeability to brine was measured after all the 5 CO_2 flooding operations (Fig. 13). In these 7 instances the permeability to brine show steeply rising trends, that did not stabilize, because the supply of brine was limited. The steeply rising trends are considered a relative permeability effect in a system where supercritical CO_2 fluid is being displaced from the pore space of the core sample by brine flow, and at the same time CO_2 is dissolved into the brine. The steeply rising permeability trends point towards the levels of the previously measured brine permeabilities at Sw=100%.

In Exp-3 and Exp-4 larger supplies of brine were available. A brine permeability measurement in Exp-3 reached 96% of the previously measured brine permeability value (Fig. 19), while a brine permeability measurement in Exp-4 was 104% of the previously measured brine permeability value (Fig. 30). Therefore Exp-3 and Exp-4 shows that the high-rate CO_2 flooding operations of these experiments did not change the permeability to brine.

Table 10. Summary of brine flooding operations.

Exper-iment id.	Flooding operation id.	Injection rate (ml/h)	RRI gas perm (mD)	Perme-ability at end (mD)	Injected brine (PV)	Characterization of general trend
Exp-1	Initial Brine	800	1177	978	4.3	Stable
	Brine #1	100	1177	450	2.6	Steeply rising
	Brine #2	100	1177	460	0.5+3.0	Steeply rising
Exp-2	Initial Brine	100	1310	1030	3.8	Stable
	Brine #1	100	1310		4.9	
	Brine #2	100	1310		6.7	
	Brine #3	100	1310		6.7	
	Brine #4	100	1310		4.1	
	Brine #5	100	1310		4.6	
Exp-3	Initial Brine #1	100	1203	1014	3.8	Stable
	Initial Brine #2	100	1203	1050	6.8	Stable
	Brine #1	100	1203	1004	15.4	Stable at end
Exp-4	Initial Brine	100	1470	1223	4.2	Stable
	Brine #1	100	1470	1275	9.3	Slightly rising

Table 11 gives a summary of the 15 CO_2-flooding operations of the four experiments.

Exp-1 used a CO_2-flooding scheme with three CO_2-flooding operations separated by three brine-flooding operations (Fig. 6). CO_2-flooding operation #3 of Exp-1 is divided in two parts by a flow reversal.

Exp-2 used a CO_2-flooding scheme with five CO_2-flooding operations separated by six brine-flooding operations (Fig. 13). An additional CO_2-flooding operation failed because of blocking of rig tubing by fines. CO_2 flooding operation #2 of Exp-2 is not considered further as it used an injection rate that did not allow determination of permeability.

Exp-3 used a CO_2-flooding scheme with one extended CO_2-flooding operations separated by two brine-flooding operations. The CO_2-flooding operation was a composite operation starting with injection of 152 PV's of CO_2 at 1740 ml/h followed by injection of 11 PV's of CO_2 at 800 ml/h (Fig. 22). This CO_2-flooding operation of Exp-3 is divided in a high-rate operations at 1740 ml/h and a low-rate operation at 800 ml/h.

Exp-4 used a CO_2-flooding scheme with two composite CO_2-flooding operations separated by two brine-flooding operations. The CO_2-flooding operations were composite operation starting with injection at 1740 ml/h followed by injection at 800 ml/h (Fig. 29).

Table 11. Summary of CO_2 flooding operations.

Exper-iment id.	Flooding operation id.	Injection rate (ml/h)	Perme-ability at end (mD)	Injected CO2 (PV)	Characterization of general trend	Characterization of trend at end	Permeability change at break
Exp-1	CO2 #1	800	180	33.5	Unstable w. 2 initial breaks	Slowly rising	-7%, -12%
	CO2 #2	800	200	21	Standard trend	Slowly rising	
	CO2 #3 initial	800	72	17.4	Unstable w. break	Stable	-75%
	CO2 #3 end	800 reversed	375	6	Standard trend	Slowly rising	
Exp-2	CO2 #1	800	355	35.4	Standard trend	Stable	
	CO2 #2	10	n.a.	20.7	No trend because low rate	No trend because low rate	
	CO2 #3	800	300	29.8	Standard trend	Slowly rising	
	CO2 #4	800	290	17	Standard trend	Rising	
	CO2 #5	800	340	29.8	Standard trend	Rising	
Exp-3	CO2 #1 High rate	1740	366	151	Unstable w. 2 spontaneous breaks and one provoked break	Slowly rising	-33,-53%,+30%
	CO2 #1 Low rate	800	306	10.7	Stable	Stable	
Exp-4	CO2 #1 High rate	1740	115	73	Unstable w. initial break	Stable	-59%
	CO2 #1 Low rate	800	162	15.9	Stable	Stable	
	CO2 #2 High rate	1740	263	72.8	Unstable w. initial break	Stable	-17%
	CO2 #2 Low rate	800	256	13.5	Stable	Stable	

Contrary to the brine permeability measurements, the characteristics of the CO_2 flooding operations are very variable. Some show a smooth permeability curve starting with a steep rise that gradually levels off. This trend is referred to as a "standard trend", which is shown by Exp-1 #2, Exp-1 #3 end, Exp-2 #1, Exp-2 #3, Exp-2 #4, and Exp-2 #5. In the instances where the flooding operation lasted long enough, it ends with a stable permeability at the end of the trend.

Five of the CO_2-flooding operations were unstable with spontaneous permeability drops that could not be correlated with rig operations like change of flow pattern or pump operation. A total of 7 such breaks were recorded (Table 11). Such instances are Exp-1 #1 (2 breaks), Exp-1 #3 initial, Exp-3 #1 High rate (2 breaks), Exp-4 #1 High rate, and Exp-4 #2 High rate. These flooding operations all display one or two abrupt drops in permeability that cannot be correlated to any external cause. In all instances the permeability is reduced by between 7% to 75%. An additional case is the third break of Exp-3 #1 High rate, where permeability increased by 30%. This case differs from the other breaks as it was probably triggered by the operation of a valve that cause an increase in fluid pressure by 0.6 bar from 199.5 bara to 200.1 bara. This permeability increase countered the permeability reduction earlier in flooding Exp-3 #1 High rate. All three high-rate CO_2 flooding operations (1740 ml/h) experienced spontaneous drops in permeability. If we only consider the cases where the flooding started at Sw=100%, only two of the seven low-rate CO_2 flooding operations (800 ml/h) experienced such permeability drops.

The 8 permeability breaks all take place in a very short time. The use of a logging interval of 2 seconds (12 seconds in the case of Exp-1) made it possible to trace the permeability changes in detail, cf. Figs. 32 and 35. In all instances the change took place within 1 minute, usually within 30 seconds. The permeability changes were not accompanied by changes in other parameters, except a change in fluid pressure by a fraction of a bar. The permeability changes always occurred at a time when the fluid density log showed an undulating trend indicative of production of small amounts of water together with the CO_2. But the changes could never be correlated with any particular irregularity in the fluid density trace.

In the case of Exp-1 #3 it was decided to reverse the flow direction in the core holder to see the effect on the permeability (Fig. 6). The flow reversal was effected at PV 78.8 to 79.3, and had the effect that the CO_2 permeability immediately increased to a level of 250 to 300 mD, which is significantly higher than the permeability at the end of the two first CO_2-flooding operations of Exp-1. Furthermore, the CO_2 permeability continued to increase to 375 mD where the CO_2-flooding stopped because the CO_2-supply was empty. At this time the CO_2 permeability was slowly rising.

Upon completion of Exp-1 fines migration was suggested to be the likely cause of the permeability breaks (Olsen et al. 2020). This is no longer suggested, because fines migration inside the core is expected to give a much slower permeability response, as it is unlikely that fines can block the whole cross section of the core in less than 30 seconds. Fines migration outside the core, causing blockage of rig tubing, was considered a possibility immediately after Exp-1. For this reason particle traps were installed inside the core holder in Exp-2, Exp-3, and Exp-4. These traps did catch some fines, but they did not prevent the four permeability breaks of Exp-3 and Exp-4. Therefore, fines migration is no longer considered the cause of the permeability breaks.

It is now suggested that channelling of CO_2 within the core samples is the cause of the permeability breaks. The viscosity ratio $\mu_{CO2}/\mu_w = 0.1$ caused the CO_2 to concentrate in channels, possibly more pronounced towards the outlet end of the core sample. At irregular time intervals the CO_2 flow within the core spontaneously changed to another position. The reason for this change is not clear. The fluid density log shows production of water from the core sample through most of the CO_2 injection periods. Probably the shift in channel position

was caused by changes in water distribution within the sample. Drying out of pores with precipitation of salt may play a role. Six of the seven instances of spontaneous permeability drop occurred before injecting more than 6 PV's of CO_2. Therefore, the probability of spontaneous drop in permeability is clearly greatest at the start of an injection operation when the water saturation is high. Also, the probability of spontaneous permeability drop appears to be higher at high injection rate (1740 ml/h) than at low injection rate (800 ml/h).

The water saturation determinations of the core plugs of Exp-4 after dismounting the samples from the experimental rig shows a strong gradient in water saturation towards the outlet end of the composite core, Fig.36. After injection of 86 PV's of CO_2 in Exp-4 CO_2 flooding #2, the core sample at the outlet end contained 65.3% of water, which is only possible if a significant part of the sample was not flooded by CO_2. Therefore, CO_2 must have flowed in channels. The water saturation data also indicates that the channelling became more pronounced towards the outlet end of the core sample. Because only 3 saturation determinations are available, the maximum water saturation found in any cross section of the composite core during the experiment was probably higher than the measured water saturation of 65.3% for sample 108.

Water saturation determinations are not available for the other experiments, but the similarity of the CO_2-flooding events suggests that CO_2 channelling took place in all the experiments, compare e.g. Exp-3 CO_2 #1 (Fig. 22) with Exp-4 CO2 #2 (Fig. 34).

4. Conclusions

CO_2-flooding experiments were conducted with samples of Nini greensand at reservoir conditions with a complex sequence of CO_2 injection and brine injection operations.

Measurements of initial permeability to brine were from 978 mD to 1223 mD, and agree with the conventional gas permeability determinations of the core samples.

Brine permeability measurements after CO_2 injection operations did not differ significantly from brine permeability measurements before injection of CO_2.

Supercritical CO_2 permeability from 72 mD to 375 mD was measured, which is from 7% to 38% of the brine permeability of the respective samples.

Events with sharp drops in permeability occurred spontaneously in seven CO_2 flooding operation on three of the four core samples. The drops in permeability were between 7% and 75% and occurred within 1 minute. In one instance flow reversal restored a significantly higher permeability. In another instance a fluid pressure change of 0.6 bar triggered a permeability increase of 30%.

After Exp-4 the three core samples of this experiment were analysed for water saturation by Dean Stark extraction. From core holder inlet towards core holder outlet, the three samples showed water saturation results of 28%, 40%, and 65%. This shows the presence of a strong water saturation gradient within the core sample from inlet towards the outlet.

It is suggested that the sharp drops in permeability are results of channelling of the CO_2 flow. The viscosity ratio $\mu_{CO2}/\mu_w = 0.1$ is the main cause of the channelling. At irregular time intervals the CO_2 flow within the core spontaneously changed to another position. The reason for this change is not clear, but movement of water and drying out of pores with precipitation of salt are possible causes. The probability of spontaneous drop in permeability is greatest at the start of an injection operation, i.e. when the water saturation is high. Also, the

probability of spontaneous permeability drop appears to be higher at high injection rate (1740 ml/h) than at low injection rate (800 ml/h).

Preliminary investigations of the core samples after the experiments do not reveal visible changes to the greensand rock.

Particles of size up to a few tenth of a millimetre were detached from the core samples and moved downstream to a particle trap situated 42 cm downstream from the core sample.

Acknowledgment

The EUDP programme is acknowledged for financial support of Project Greensand. The Project Greensand consists of a consortium of GEUS, INEOS, Maersk Drilling and Wintershall DEA.

References

Bloomfield, J.P., Williams, A.T. 1995. An empirical liquid permeability – gas permeability correlation for use in aquifer properties studies. *Quarterly Journal of Engineering Geology, **28**, S143-S150, 1995.*

Kestin, J., Khalifa, H.E., Abe, Y., Grimes, C.E., Sookiazian, H., Wakeham, W.A. 1978. The effect of pressure on the viscosity of aqueous NaCl solutions in the temperature range 20-150 °C. *J. Chem. Eng. Data **23,4**, 328-336, 1978.*

MacDonald, I., Mair, K. 2003. Nini-4. Conventional core analysis report. Nini-4 (5605/10-1). Licence 4/95. *Robertson Research International Ltd. Report no. AF790, March 2003.*

Olsen, D., Holmslykke, H.D., Weibel, R., Schovsbo, N. 2020. Setup and sample program of CO_2 experiments. Greensand Phase 0. *Danmarks og Grønlands Geologiske Undersøgelse*, rapport 2020/19.

Olsen, D., Mohammadkhani, S., Weibel, R., Schovsbo, N.H. 2020. Preliminary results of CO2-flooding experiment Exp-1. Greensand Phase 1 WP2. *Danmarks og Grønlands Geologiske Undersøgelse*, rapport 2020/54.

NIST Chemistry Webbook: National Institute of Standards and Technology, www.webbook.nist.gov/chemistry. 2020.